DEEP SUBWAVELENGTH PATTERNING VIA ABSORBANCE MODULATION

by

Rajakumar Varma Manthena

A thesis submitted to the faculty of
The University of Utah
in partial fulfillment of the requirements for the degree of

Master of Science

Department of Electrical and Computer Engineering

The University of Utah

August 2011

Copyright © Rajakumar Varma Manthena 2011

All Rights Reserved

The University of Utah Graduate School

STATEMENT OF THESIS APPROVAL

This thesis of **Rajakumar Varma Manthena**

has been approved by the following supervisory committee members:

Rajesh Menon, Chair — **05/23/2011** Date Approved

Carlos Mastrangelo, Member — **05/23/2011** Date Approved

Steve Blair, Member — **05/23/2011** Date Approved

and by **Gianluca Lazzi**, Chair of the Department of **Electrical and Computer Engineering** and by Charles A. Wight, Dean of the Graduate School.

ABSTRACT

Creating very small structures in the resist exceeding diffraction limit is becoming a bottle-neck in lithography especially for nanoscale features. A novel optical lithography technique that has the ability to overcome the diffraction barrier is *Absorbance Modulation Interferometric-Lithography (AMIL)*. Feasibility of this technique is experimentally verified. In this approach of absorbance modulation, a standing wave at wavelength λ_2 (633nm) is overlaid with a uniform beam from a light-emitting diode with a center wavelength at λ_1 (310nm). Both beams illuminate a photoresist film overcoated with a photochromic layer. This photochromic layer localizes the transmitted light at λ_1 to subwavelength spatial dimensions. The subwavelength lines are spaced by a diffraction-limited grating period. In order to generate dense lines, the sample is mounted on a single-axis high precision scanning stage that will enable multiple exposures.

To my advisor, Rajesh Menon

CONTENTS

ABSTRACT . . . . **iii**

LIST OF FIGURES . . . . **vii**

LIST OF TABLES . . . . **ix**

ACKNOWLEDGEMENTS . . . . **x**

CHAPTERS

1. INTRODUCTION **1**

1.1 Motivation 2
1.2 Maskless Lithography Techniques 3
1.2.1 Scanning-Electron-Beam Lithography (SEBL) 4
1.2.2 Focused Ion Beam (FIB) 4
1.2.3 Multiple Electron Beam 5
1.2.4 Scanning Probe Lithography (SPL) 5
1.3 Related Work 5
1.3.1 Zone-Plate-Array Lithography (ZPAL) 6
1.3.2 Patterning via Optical-Saturable Transitions (POST) 6
1.4 Thesis Overview 9

2. BACKGROUND **11**

2.1 Interferometric Lithography 11
2.2 Interferometric Lithography Using Absorbance Modulation Technique 12
2.3 Absorbance Modulation Layer (AML) 15
2.3.1 Bithienylethene (BTE) 16
2.3.2 Diarylethene Polymer 17
2.3.3 Absorbance Plots of Photochromic Molecules 18
2.4 MATLAB Simulations - Power Reflectivity 29

3. ABSORBANCE MODULATION INTERFEROMETRIC-LITHOGRAPHY (AMIL) **36**

3.1 Experimental Setup 36
3.2 Layers in the Sample Stack 37
3.3 Sample Preparation 38
3.3.1 Antireflection Coating (ARC) 39
3.3.2 Photoresist 39
3.3.3 Polyvinyl Alcohol (PVA) 40

3.3.4 Photochromic Molecules 41
3.4 PVA Roughness Analysis 42
3.5 Experimental Results 44
3.5.1 BTE as Absorbance Modulation Layer 44
3.5.2 Diarylethene Polymer as Absorbance Modulation Layer 48
3.5.3 Linewidth *vs.* Dose 50

4. CONCLUSIONS 53

4.1 Summary 53
4.2 Future Work 54
4.2.1 New Setup with High Power Sources 54
4.2.2 Other Photochromic Molecules that Have Even Better Absorbance Contrast 55
4.2.3 Use of Chemically Amplified Resist 55
4.2.4 More Multiple Exposures 55
4.2.5 AML that Does Not Affect the Resist 55
4.2.6 Pattern Transfer 56

REFERENCES 58

LIST OF FIGURES

1.1 Schematic of Zone Plate Array Lithography(ZPAL) 7

1.2 Schematic illustrating the photochemical transformations in the POST approach 8

2.1 Schematic illustrating the sinusoidal intensity pattern formed by the interference of two coherent beams 12

2.2 Schematic illustrating formation of aperture in AMIL approach 13

2.3 Schematic explaining how to do double exposure with AMIL. 14

2.4 Increasing power density at λ_2 relative to λ_1 squeezes the transmitted spot, *i.e.,* nanoscale optical probe 15

2.5 Open(opaque) and closed(transparent) molecular forms of Bithienylethene (BTE) 16

2.6 Diarylethene polymer (single molecule) in its open and closed forms . . . 17

2.7 UV-Vis spectrum of Bithienylethene (BTE). 19

2.8 Absorbance of BTE *versus* time in minutes corresponding to wavelengths λ_1 and λ_2 during the transition from closed to open form. 21

2.9 Composition of diarylethene polymer in open and closed forms. 22

2.10 The UV-Vis spectrum of diluted diarylethene polymer. 24

2.11 The UV-Vis spectrum of diarylethene molecules used for AML. 25

2.12 UV-Vis spectrum of BTE used in *POST* during its transition from open to closed form. 26

2.13 UV-Vis spectrum of BTE used in *POST* during its transition from closed to open form. 27

2.14 Absorbance of BTE at 310 nm and 633 nm during its transition from open-close and close-open forms. 28

2.15 Absorbance of BTE at λ_2=633nm during its repetitive transitions between open-close forms. 29

2.16 2D MATLAB simulation of power reflectivity at the interface of antireflection coating and photoresist layer 31

2.17 1D MATLAB simulation of power reflectivity with either antireflection coating or photoresist layer thicknesses as a variable in the stack. 32

2.18 2D MATLAB simulation of power reflectivity with antireflection coating and thickness of the Platinum layer as variables 34
3.1 Schematic of AMIL approach 37
3.2 Recent AMIL experimental setup with piezo-controlled nanoprecision stage controllable by LabVIEW 37
3.3 Schematic of AMIL sample with all the layers in the stack 38
3.4 AFM images of PVA layer corresponding to different concentrations and ways of curing 43
3.5 AFM images of different *AMIL* exposures with BTE as AML 45
3.6 SEM images of *AMIL* exposures (thin resist = 70nm) with BTE as AML 46
3.7 More AFM images of *AMIL* exposures with BTE as AML 47
3.8 AFM images of *AMIL* exposures with Diarylethene polymer as AML . . 49
3.9 Graph corresponds to line width versus single *AMIL* exposure dose . . . 50
3.10 AFM images of different *AMIL* exposures with same intensity ratio of λ_1 and λ_2, period of the grating is 650nm 51
4.1 Pattern transfer outline. The purpose of the Silicon-dioxide layer is to transfer the pattern onto ARC. 57

LIST OF TABLES

3.1 Linewidth *vs.* exposure time of a single AMIL exposure. 52

ACKNOWLEDGEMENTS

It has been only two years since I started my Graduate School journey at the University of Utah but it is infrangible, my relation with the school. Even though I had course work in the Master's, most of the technical and practical knowledge is gained from exposure to different aspects of research especially through this thesis. This section will not be sufficient to express my gratitude to my advisor, Rajesh Menon. From my personal experience, Menon is the ideal advisor one can expect to have. I am lucky to have him as my advisor and also to be his first graduate student. Apart from giving proper guidance, he encouraged me a lot in each and every aspect of my Master's career. He was very helpful and patient in improving my writing skills in particular. The most important of all are his great personal qualities that I picked up in this course of time.

I would like to thank professors Carlos Mastrangelo and Steve Blair for serving as my committee members, and also for providing their valuable comments and suggestions at every stage. Blair in particular was very co-operative and helpful by giving his thoughtful feedback at various phases of this research. Nicole Brimhall, Mohit Diwekar and Amarchand Sathyapalan who are Post Docs in our group with whose co-operation I was able to do all this starting from scratch. I really enjoyed working with them and also I learned a lot from these guys.

A few other people in Nano Fab and Surface Analysis Laboratories at the University of Utah to whom I am very grateful in particular are Brian Van Devener, Brian Baker and Charles Fisher. These people too played a indirect role in the success of this thesis.

Thanks to Utah Science, Technology and Research (USTAR) Initiative, Defense Advanced Research Projects Agency (DARPA) and National Science Foundation (NSF) for having faith in this research and supporting this research for several years.

I thank my parents for providing constant encouragement and motivation without having any clue about what I was up to. I do not think that I would have completed my graduate studies successfully without their blessings and support. Last but not least, I would like to thank my dearest lab mates Jason Edward Kleinschmidt, Ghanghun Kim and Precious Cantu for making our lab a wonderful place to work. Special thanks to all my friends in Utah especially Sandeep Chalasani and Satish Batchu for helping me take the right decisions with their valuable insights.

CHAPTER 1

INTRODUCTION

Creating pattern on the resist can be categorized into two pathways in lithography. It can be either direct, *maskless lithography* (e.g., *e-beam* or *ion beam lithography*, etc.) or indirect, generating *mask* initially and then transferring the pattern on the mask onto resist. In *photolithography*, light is the purpose of transferring a pattern onto light-sensitive chemical *photoresist* or in simple *'resist'*. A series of chemical treatments then actually creates the desired pattern on the resist. Depending on fabrication process and circuit complexity, this lithography technique is repeated several times. This shows us how important this process is in terms of repeatability and reliability in the fabrication process. General requirements of current or future lithography systems are to create dimensions in a few tens of nanometers, very small variation in dimensions, i.e., very good line width control, accurate alignment of subsequent pattern, low distortion of image and sample, high throughput, i.e., low cost, high reliability, uniformity over large areas, etc. In most commercial fabrication processes, *photolithography* is done through exposure systems that use mask instead of direct exposure systems because of major factors like cost and bulk production of chips.

Exposure systems that use mask create pattern on the wafer using a *photomask* by shining a uniform light on it. Photomask blocks the light in some areas and lets it pass in the other areas. Exposure systems that use mask are further classified based on the optics that transfers the image from the mask onto the wafer. One of them is *contact* or *proximity* lithography. In this technique, photomask is placed in direct contact with the wafer or with a small gap between the photomask and wafer, respectively. Here the wafer is completely covered by mask when it is exposed to a uniform light at certain intensity based on the resist and its characteristics. *Projection lithography*

is the other exposer system that uses masks to create pattern where projection masks show only one or an array of dies. It is a most common technique in *Very-large-scale integration (VLSI)* lithography projecting mask onto a wafer many times to create the entire pattern.

1.1 Motivation

Projecting clear image of smaller features onto the wafer is limited by the wavelength of the light that is used for exposure and also the optical systems used to capture enough diffraction orders from the illuminated mask. To create feature sizes down to 50nm, *deep ultraviolet (DUV)* light from the lasers having peak wavelengths of 248nm and 193nm was used until recently, and also continued improvement in lithography played a crucial role in withholding *Moore's Law* for the past 20 years [1, 2, 3]. Industries have to focus on reducing emission light wavelength of the lasers [4-5] to improve the resolution limits in photolithography.

Abbe diffraction limit: Exact spacing in the specimen can be resolved when the numerical aperture of the objective lens is large enough to capture the first order diffraction pattern produced in diffraction limited microscope at a specific wavelength

$$AbbeLimit(d) = \frac{\lambda}{2 \times NA_{obj}} \tag{1.1}$$

where,

d = lateral resolution, λ *= wavelength, n = smallest refractive index in the optical path,* NA_{obj} *= numerical aperture of objective =* $n \times sin \frac{1}{2} A$*, A= Angular Aperture of a cone of light entering the lens, n = smallest refractive index in the optical path*

Shorter wavelengths, better lenses, and adaptive optics have all contributed to this Law, which has allowed commercially available chips to be fabricated with 45nm, 32nm and 25nm [6] feature sizes. These processes had succeeded beyond everyone's expectations on the small feature lithography, but at the same time, this does not mean that future feature reductions that rely only on this technology (or) with this technology are guaranteed. Approaches that claim to allow this are so-called maskless

lithography which saves manufacturers tens of thousands of dollars each time a change is made in device design, no matter how large or small the change is.

Looking at both masked and maskless photolithography technologies, the maskless part is also gaining a lot of importance these days. Normal lithography creates an image of the features that will be etched into a chip by imaging a negative mask, which in most cases mask is in contact with the resist onto which the feature is to be transferred. Usually these masks are big in size, very expensive for long term usage, and can take quite a while to make depending on the features. When you are just trying to get a chip design right, each little change means a new mask. You can imagine that this might increase the development cost somewhat, while also slowing circuit development.

Maskless lithography partially eliminates these problems by writing or creating pattern on the chip directly, which does not require any physical or proximity contact of mask. This can be done by milling the silicon with a beam of electrons, ions or photons. Electrons and ions can be focused to very small spots, meaning that features just a few nanometers in size can be written, but this is a seriously slow way to write an entire chip. Running many beams in parallel would speed the process up. Unfortunately electrons and ions are charged, so the beams interact with each other: parallel beams do not focus, and do not go where they are directed. Light, on the other hand, does not interact so strongly with itself, making it the perfect candidate for maskless lithography.

1.2 Maskless Lithography Techniques

There are various forms of maskless lithography, mainly Scanning Electron-Beam Lithography (SEBL), Focused Ion-Beam (FIB) Lithography, Multi-Axis Electron-Beam Lithography (MAEBL), Interference Lithography (IL), Maskless Optical-Projection Lithography (MOPL), Zone-Plate-Array Lithography (ZPAL), Scanning-Probe Lithography (SPL), Dip-Pen Lithography (DPL), etc.[7].

1.2.1 Scanning-Electron-Beam Lithography (SEBL)

Scanning-Electron-Beam Lithography (SEBL) is a practice of scanning a beam of electrons in a predefined fashion (desired pattern) across a surface covered with a resist and then removing either exposed or unexposed regions of the resist (also known as *developing the resist*). The major advantage associated with SEBL is that it overcomes the diffraction limit of light and makes features in the nanometer regime which had found vast recognition in making photo masks used in photolithography, only low volume production of semiconductor components, and in Research and Development (R&D). But then, its limitation is throughput, i.e., it takes a very long time, even several days in some cases, to expose an entire silicon wafer with photoresist, which means it is easily vulnerable to beam drift or instability which can be partially eliminated with other techniques [8]. Other defects include sample charging, backscattering calculation errors, dose errors, fogging (long-range reflection of backscattered electrons), contamination and resolution limits based on resist [9].

1.2.2 Focused Ion Beam (FIB)

Focused Ion Beam (FIB) Lithography has many advantages over the electron beam counterpart in terms of resist sensitivity, backscattering and proximity effects. Applying the Top Surface Imaging (TSI) principal to FIB lithography could further enhance its capability [10]. Even though FIB systems are capable of very high resolution, they suffer from worse problems of throughput and placement accuracy than SEBL systems as well. Interference Lithography has many forms [10-13] and throughput is quite high. However, it is applicable only to periodic and quasi-periodic patterns, where it excels. SPL [14] and DPL [15] have a number of unique aspects and play an important role in nanostructures research. However, they do not appear to have the general applicability of optical lithography techniques and lack sufficient throughput for applications outside of research. A *MOPL* system has been proposed that replaces the mask with a programmable micromirror array [16-17].

1.2.3 Multiple Electron Beam

Multiple electron beam (multibeam) approaches [19], [20] and [21] offer a high throughput solution for sub-100nm lithography when compared to single-beam[18]. It is very difficult to obtain throughput in a single-beam *electron-beam lithography(EBL)* due to electron-electron interaction which limits lithography resolution by increasing fuzz in the beam current, whereas resolution is directly proportional to the total beam current supplied to expose the given resist. The use of a multibeam approach can result in compared to singlebeam approach throughput while maintaining pattern accuracy and quality. In multibeam approach, the current in each beam can be considerably reduced and at the same time, a high total current can be maintained at the wafer surface. Two major applications of multibeam are direct-write-on-wafer and maskmaking. Also multibeam approach eliminates the maskmaking, resulting in reduced costs and effects from the masks in the semiconductor IC manufacturing process.

1.2.4 Scanning Probe Lithography (SPL)

*Scanning Probe Lithography (SPL)*is a type of maskless lithography that is based on Scanning Probe Microscopy(SPM), in which nanoscale features are constructed on the wafer surfaces by drawing lines directly either by removing atoms from a passivated silicon or by touching the target surface with a Scanning Probe Microscopy tip that has been loaded with a chemical substance which needs to be patterned on the surface. The latter technique is also known as *Dip Pen Lithography (DPL)*. In both the approaches, the probe is moved in a raster scan manner of the specimen, i.e., line by line and then recording the probe to surface interaction as a function of position. Resolution in atomic scale can be achieved with the advent of piezoelectric actuators to execute motions with a very high precision and accuracy.

1.3 Related Work

This section presents two techniques - *Zone-Plate-Array Lithography (ZPAL)* and *Patterning via Optical Saturable Transitions (POST)* that are influential or related to *AMIL*.

1.3.1 Zone-Plate-Array Lithography (ZPAL)

In *Zone-Plate-Array Lithography* [14], an array of diffractive lenses (e.g., Fresnel zone plates) focuses an array of spots on the surface of a photoresist -coated substrate. The light intensity of each spot is controlled by one element on a spatial light modulator (SLM). The substrate is scanned on a high precision stage while the elements of the SLM are appropriately controlled, resulting in patterns of arbitrary geometry being written in a 'dot-matrix' fashion. A schematic of ZPAL is shown in Fig. 1.1. The light source is preferably a continuous wave (CW) laser (a pulsed laser source would severely limit system throughput). Light from the laser is passed through a spatial filter and a collimating lens to create a clean, uniform beam incident on the SLM. The SLM breaks the beam into individually controllable beamlets. A telescope is placed such that each beamlet is normally incident on one zone plate in the array. A Fourier filter within the telescope ensures that there is sufficient contrast between the on and off states. It also prevents cross talk between the beamlets. Each zone plate behaves like a microscopic lens focusing the light into a tight on-axis spot in its focal plane.

Alternate zones of the zone plate can either block the transmitted radiation or phase shift it. The former are called *'amplitude zone plates'* and the latter *'phase zone plates'*. Phase zone plates have much higher focusing efficiency ($\sim$40%) than amplitude zone plates ($\sim$10%), whereas phase zone plates are also assumed to consist of circular, concentric zones of alternating π and 0 phase shifts [3]. The radii of the zones are chosen such that there is constructive interference at the focus.

1.3.2 Patterning via Optical-Saturable Transitions (POST)

Patterning via Optical-Saturable Transitions (POST) is an approach similar to *Absorbance Modulation Interferometric Lithography* (described later in this paper) that is based on spectrally-selective reversible and irreversible photochemical transitions. POST involves the use of molecules that reversibly change their absorbance spectra upon irradiation [15]. These molecules exist in two isomeric forms.

As shown in Fig. 1.2, when the form A (e.g., an open bond) is irradiated by photons of wavelength, λ_1, they transform into form B (e.g., a closed bond). When

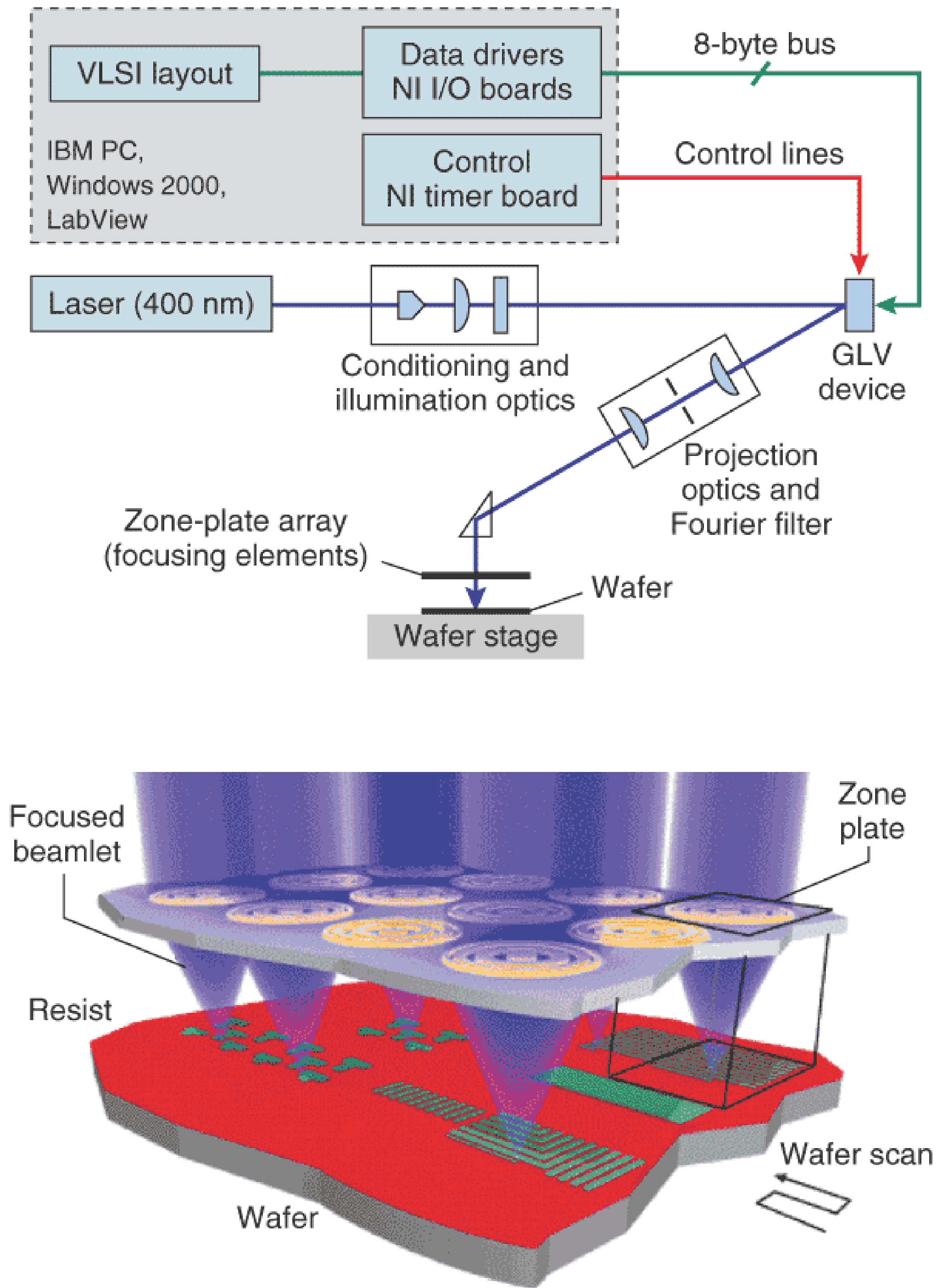

Figure 1.1: Schematic of Zone Plate Array Lithography(ZPAL)

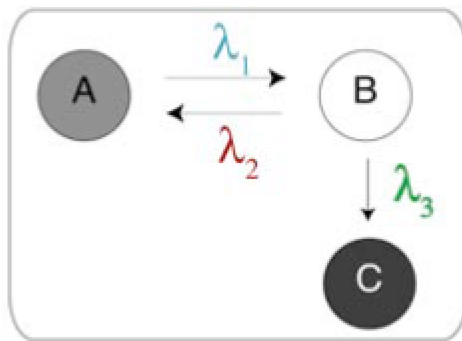

Figure 1.2: Schematic illustrating the photochemical transformations in the POST approach

the form B is irradiated by photons of wavelength, λ_2, they transform back to form A. If in addition, form B can be transformed irreversibly via exposure to photons at wavelength, λ_3 into a highly stable form C (which is feasible for certain organic molecules), and single-molecule resolution in 3-D is achievable.

In the POST implementation, molecules that undergo reversible transitions at λ_1 and λ_2, and an irreversible transition at λ_3 are photochromic molecules, which have been extensively studied in the past for optical memories, molecular switches and molecular motors.

POST enables patterning at sub-10nm length scales with long-wavelength photons. Earlier, nanostructures could only be patterned by focused electron beams, ion beams or very short-wavelength photons. These particles can cause damage to many types of substrates and also they require vacuum and hence are incompatible with fragile organic samples which are complex and expensive. Many approaches were proposed to overcome these problems. A large array of independently controlled nodes enables rapid patterning ($\lambda/8$) via *POST*. Large depth of- focus can be engineered into 2-D nodes enabling very robust 2-D patterning with large process latitude. Furthermore, the potential to rapidly create nanostructures in 3 dimensions with low power visible and near-UV wavelengths will revolutionize nanomanufacturing. But the most important limiting factor of this technique, even though it could be able to overcome the Abbe diffraction limit, is that the resist here is not commercially available photo resist, whereas most of the current fabrication processes are based on commercially

available photo resists either positive or negative based on the application. In some cases, different kinds of photo resists regardless of their availability (cost perspective) are used, say for example, high aspect ratio, and very short exposure time, complex structures, etc. *Absorbance Modulation Interferometric-Lithography (AMIL)* is an alternative to *POST* that overcomes the diffraction barrier which is a major concern in the current lithography techniques.

1.4 Thesis Overview

The rest of this thesis is organized as four chapters which give a detailed description of the contributions of this research.

Chapter 2 describes Interferometric Lithography technique in particular based on absorbance modulation, characterization of materials in the stack of four layers used in the current *Absorbance Modulation Interferometric-Lithography(AMIL)* research technique and also the preparation of each layer in the stack, Absorbance of Photochromic molecules corresponding to *Bis-bithienylethene (BTE)* developed by Trisha Andrew from Massachusetts Institute of Technology (MIT) and also of *Diarylethene* polymer from Italy, in its closed and open forms at different wavelengths. Photochromic material can be translated between its open and closed forms based on the time duration the material is exposed to a specific wavelength either λ_1=310 nm (or any Ultra Violet Source) most cases the UV source for this test is Xenon-Arc Lamp, sometimes using UV LED having peak wavelength at 310 nm or λ_2=633 nm (He-Ne Laser). Surface roughness of all the layers in the material stack is discussed individually, *polyvinyl alcohol (PVA)* in brief. PVA is a blocking or protecting layer on top of photo resist to prevent photochromic molecules from attacking the resist. Also discussed are MATLAB simulation results showing reflectivity *versus* material thickness in the stack of four layers, varying ARC and photoresist thickness in particular.

Chapter 3 presents the canonical experimental setup of proposed research *Absorbance Modulation Interferometric-Lithography (AMIL)* with nanoprecision piezoelectric-controlled stage and different UV Wavelength sources. Nanoprecision stage is controlled by USB interface to a Personal Computer through LabVIEW software. Fab-

rication of the sample with all the four layers on which *AMIL* is performed is shown. Also discussed is more about results of this *AMIL* research with *Atomic Force Microscopy (AFM)*, *Scanning Electron Microscopy (SEM)* and Optical images corresponding to various *AMIL* exposures performed on different kinds of positive and negative resist samples, with both types of photochromic materials Bis-bithienylethene (BTE) and Diarylethene polymer at different intensity ratios of two wavelengths λ_1 = 310 nm or 325 nm and λ_2 = 633 nm. In order to minimize the exposure dose, chemically amplified positive resist is also used. Considering the resolution effect *w.r.t* resist layer thickness, resist layer thickness in the four layers stack is thinned down considerably. Linewidth of the grating due to *AMIL* exposures *versus* Exposure dose of *Shipley S1813* positive resist is also presented.

Chapter 4 summarizes the research work detailed in this thesis. The scope of this research is also presented. This chapter also describes a number of interesting areas where this research is applicable directly or indirectly in the current fabrication lithography. While this work solves some of the problems related to miniature nano-repetitive patterning, there are numerous interesting problems that still need to be overcome. The future work section of this chapter describes some such problems which need to be addressed.

CHAPTER 2

BACKGROUND

In most commercial processes, Photolithography (also known as optical lithography) means to create pattern on the wafer using photomask. Even though it is the simplest and most cost effective way to create pattern on the resist, it is severely limited by many parameters. Especially, features are limited by the wavelength of the light that is used. Absorbance Modulation Interferometric Lithography (AMIL) is a novel optical lithography technique that has the ability to overcome this diffraction limit. This AMIL technique, as explained in Chapter 1, is also based on a reversible photochemical transition. It involves usage of the molecules that reversibly change their absorbance spectra upon specific irradiation. The photochromic molecules used in this approach are Bithienylethene (BTE)and Diarylethene polymer.

2.1 Interferometric Lithography

Interference Lithography (IL) is implicitly limited when compared to many other lithography techniques. Through IL only periodic pattern can be produced which is very advantageous to fabricate devices that need a periodic pattern. IL technique used in this research uses only two beams, producing a periodic pattern in only one dimension. Exposing this pattern on a substrate with photoresist creates a set of parallel lines due to highly nonlinear dissolution rate as a function of dose. Often these parallel lines are known as *grating* as shown in Fig. 2.1.

The intensity pattern formed using interference lithography is sinusoidal; the amplitude and periodicity of the sinusoid are the only lithographic parameters that can be altered in this technique. Nonperiodic patterns are impossible to create using interference lithography alone. Also, creating periodic pattern in more than one dimension demands more than two interfering beams or more than one exposure

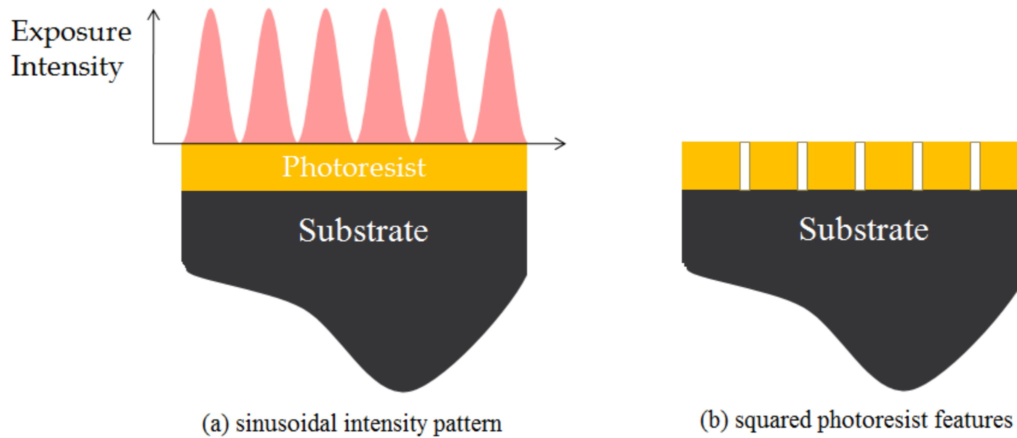

Figure 2.1: Schematic illustrating the sinusoidal intensity pattern formed by the interference of two coherent beams

based on the requirement. The range of devices which can be made using *IL* is limited; a few examples are patterned magnetic media and distributed-feedback lasers. However, interference lithography is the best, and often the only lithographic option for periodic devices because most of the other lithography techniques cannot attain the spatial-phase coherence of a truly periodic structure, producing at best only quasi-periodic structures. Another advantage of this interference lithography is its ability to make smaller features than any other optical scheme at a given wavelength.

The minimum linewidth (half-pitch)of grating l_{min} in optical lithography is often given in the form of Equation 1.1. Most advanced industrial tools maintain half-pitch of $\sim$0.53 λ. For this they are spending millions of dollars just on the lithography systems and masks, and thus it is impossible to adapt in research and university environments. Most of the affordable optical lithography tools guarantee up to $>1\mu$m resolution. With interference lithography half that of even state-of-the-art industrial systems can be achieved [22].

2.2 Interferometric Lithography Using Absorbance Modulation Technique

In this *Absorbance Modulation Interferometric Lithography* approach, a sample with *absorbance-modulation layer (AML)* on the top of photoresist is exposed to a

standing wavelength λ_2= 632.8nm, uniform beam of short wavelength λ_1 = 310 nm (LED) or 325 nm (HeCd Laser). When the AML is exposed to only wavelength λ_2, it remains in a high absorbing configuration A. Similarly if the AML is exposed to only wavelength λ_1, it attains low absorbing configuration B. When both the wavelengths are incident simultaneously, the focal ring at λ_2 super imposed by the round spot at λ_1 creates a localized subwavelength transparent aperture on the absorbance-modulation layer as shown in Fig. 2.2.

Through these transparent apertures, light with wavelength λ_1 at the nodes of λ_2 penetrates through AML and exposes the photoresist, whereas in the portions where AML is opaque, i.e., in state B, it prevents the light from passing. Once the underlying photoresist is exposed, if we turn off the light of wavelength λ_1, the AML can either thermally return to its original configuration A or it can be brought back to the high absorbance configuration B by exposing the layer to only a beam with wavelength λ_2 in case of doing multiple exposures. In general, commercially available photoresist is of a kind that it is exposed only at λ_1 but not at λ_2. Thus *AMIL* is a most feasible technique of its kind.

The way of doing double exposure with *AMIL* is shown in Fig. 2.3. After the first exposure, the sample can be moved with the help of piezoelectric nanopositioning stage (for high precision capability) and then the AML is allowed to recover back to

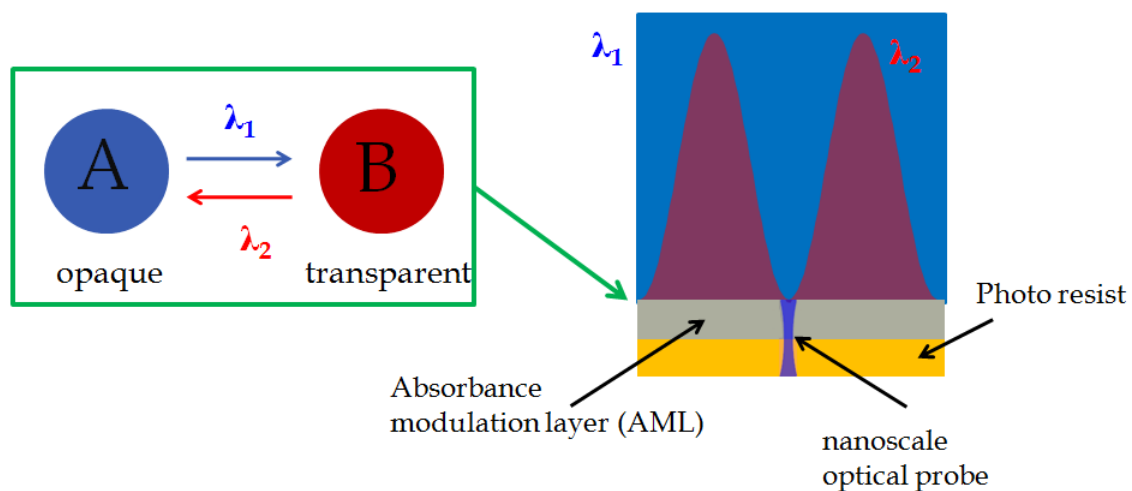

Figure 2.2: Schematic illustrating formation of aperture in AMIL approach

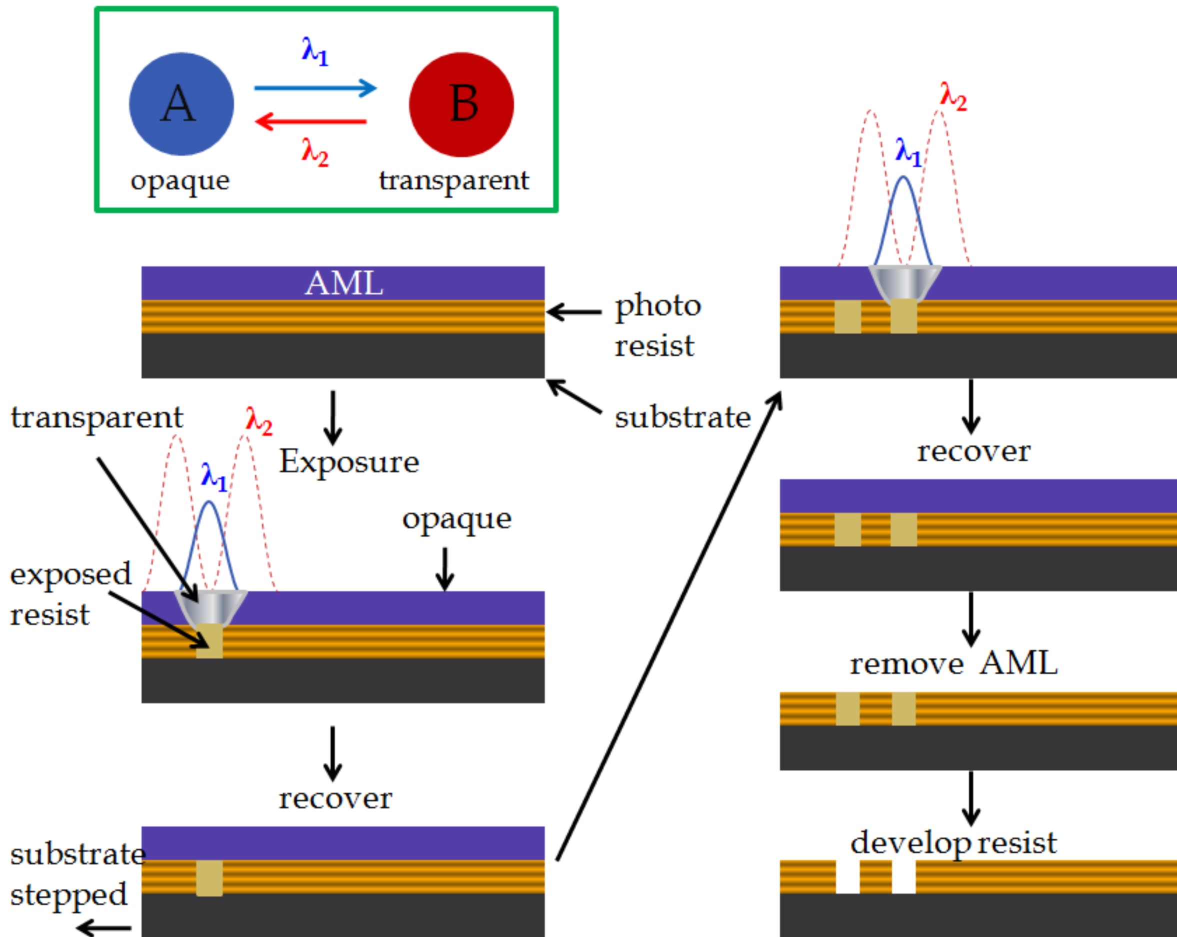

Figure 2.3: Schematic explaining how to do double exposure with AMIL.

The ring illumination at λ_2 creates a local subwavelength aperture for λ_1, through which the underlying photoresist is exposed. After exposure, the AML recovers by exposure to λ_2 or thermally. The substrate is stepped, and the λ_1, λ_2 exposure is repeated, effectively scanning the subwavelength aperture [23].

form A. This can be done either thermally or by exposing the AML to only λ_2. Once AML is completely recovered, simultaneous exposure with λ_1, λ_2 is repeated.

Standing-wave illumination at λ_2= 632.8 nm creates a local aperture at λ_1 = UV wavelength, through which underlying photoresist is exposed, whereas the size of this aperture is controlled primarily by the ratio of the intensities of the two wavelengths (in this case $\frac{\lambda_2}{\lambda_1}$), but not by individual wavelength source or optics. Hence, size is not limited to *diffraction limit* levied by either of the two wavelengths, which is a limiting issue/concern in conventional lithography techniques.

As shown in Fig. 2.4, if the ratio of intensities of $\frac{\lambda_2}{\lambda_1}$ increases, then the size of the subwavelength aperture is even narrowed, creating nanoscale features/grating($< \frac{\lambda}{10}$) exceeding the diffraction barrier (Abbe Diffraction limit) explained in Chapter 1. The size of the aperture can be controlled secondarily with the exposure dose without changing the intensity ratios by simply doing exposures that lie in between underexposed and overexposed categories. Of course a lot of calibration is needed every time the intensity ratio of two wavelengths are varied. More explanation with plots is provided in Chapter 3.

2.3 Absorbance Modulation Layer (AML)

According to *Absorbance Modulation Interferometric Lithography* technique, this section details the key layer, *Absorbance Modulation layer (AML)* in the stack of four layers on top of Silicon substrate. We described two photochromic molecules *Bithienylethene (BTE)* and *Diarylethene Polymer*, their response or states corresponding to two wavelengths. Also, their absorbance plots are presented in section 2.3.3 by spin coating each of them on a glass slide, irradiating with a Xenon

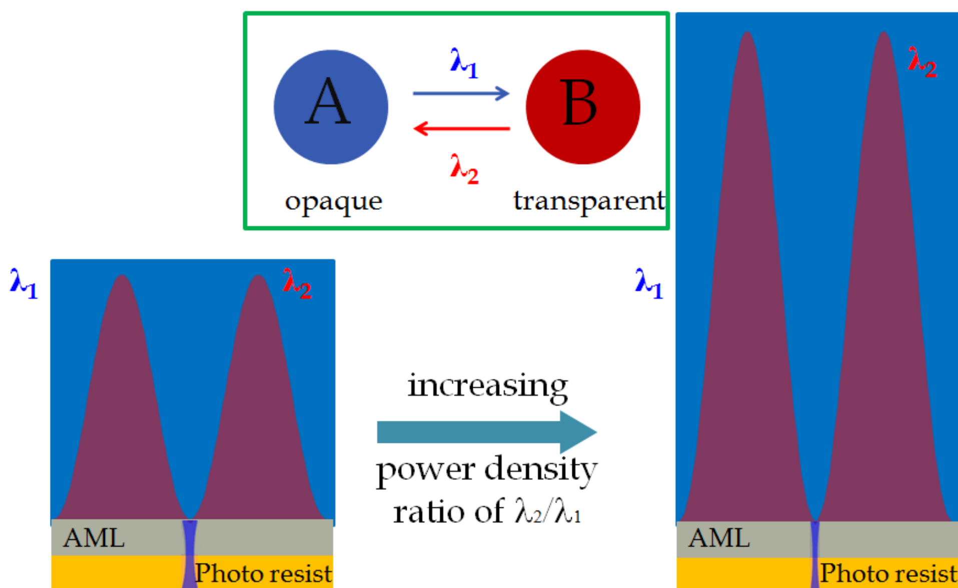

Figure 2.4: Increasing power density at λ_2 relative to λ_1 squeezes the transmitted spot, *i.e.,* nanoscale optical probe

Arc lamp, UV LED having peak wavelength at 310 nm or laser light, and conducting UV-Vis spectroscopy. The choice of wavelengths was restrained by the available lines of the Xenon Arc lamp and laser sources we have. In Chapter 3, we experimentally demonstrated the exposures with these photochromic materials. Details of the similar photochromic material similar to the one used in section 2.3.1 are also used for *POST* which will be discussed in Chapter 4.

2.3.1 Bithienylethene (BTE)

As shown in Fig. 2.5, the BTE molecules are initially present in the open form A (opaque Configuration). They are converted into closed form B (transparent Configuration) when it is irradiated by photons of wavelength, λ_1 = UV (310 or 325 nm). When the form B molecules are irradiated by photons of wavelength, λ_2 = 633 nm, they transform back to form A. This single transition is sufficient for this AMIL in case of single exposure when compared to contiguous double transitions in the POST approach of the same molecule. At the same time for a double exposure, complete reverse transition to form A has to be done before starting the second exposure.

In order to do multiple exposures or to create complex structures, we have to do the transition from open form A to closed form B and then back to form A, so on for several times. Transformation of the chemical species between two forms by the absorption of electromagnetic radiation, where the two forms have different absorption spectra, is known as *photocromism*. Absorbances of this BTE during its open and

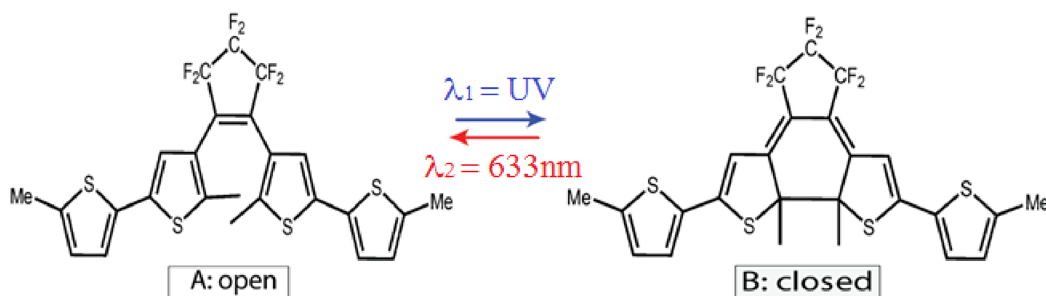

Figure 2.5: Open(opaque) and closed(transparent) molecular forms of Bithienylethene (BTE)

closed forms of photocromism are presented in subsection 2.3.3. Also presented are the saturated absorbance values *w.r.t* time, at the wavelengths λ_1 = 310 nm and λ_2 = 633 nm.

2.3.2 Diarylethene Polymer

Schematic of a single molecule in Diarylethene polymer is shown in Fig. 2.6. Like *BTE*, when these molecules are in open form A (opaque to λ_2 = 633 nm), they can be converted into closed form B (transparent configuration to λ_1 = UV (310 or 325 nm)) by irradiating with photons of wavelength, λ_1. To convert them back to form B, they are irradiated with photons of wavelength, λ_2. Based on the number of repetitive exposures, this transition between the forms is repeated. In chemistry, this phenomenon of different structural formulas at different stages, but having the same molecular formula, is known as *isomerization*.

Reversible isomerization of this polymer can also be achieved thermally. But we did not try in this research. The diarylethene polymer is also of interest for the fact that their isomerization requires very little change of shape. This means that their isomerization takes place more quickly than with most other photochromic molecules. In some cases, this photochromic behavior can be carried out in a single crystal without disrupting the crystal structure.

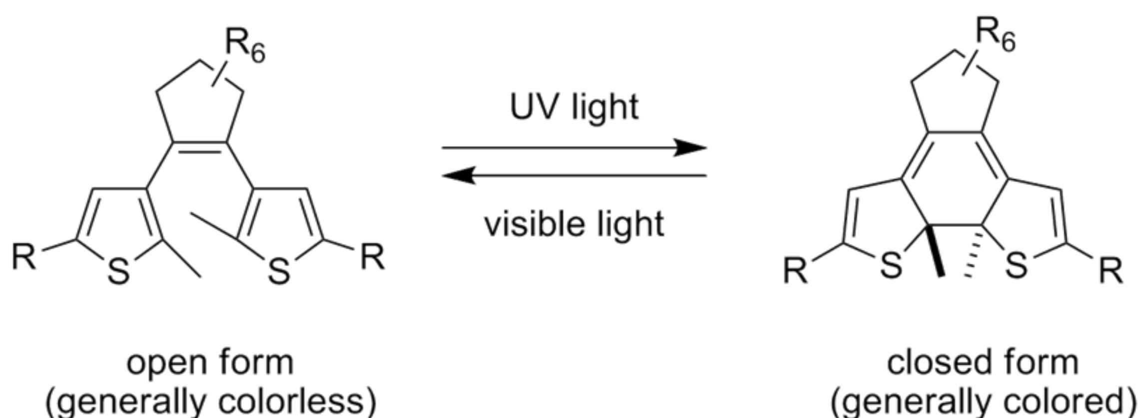

Figure 2.6: Diarylethene polymer (single molecule) in its open and closed forms

This open-ring isomer is a colorless compound, whereas the closed-ring isomer have colors dependent on its chemical structure, due to the extended conjugation along the initial molecular structure. Therefore many diarylethenes have photochromic behavior both in solution and in solid state. Also, the two isomers of this diarylethene polymer differ from one another not only in their absorption spectra explained in subsection 2.3.3, but also in various physical and chemical properties, such as their refractive indices, dielectric constants, and oxidation-reduction potentials. These properties can be readily controlled by reversible isomerization between the open and closed forms using photoirradiation to UV and visible light, and thus they have been suggested for use in optical data storage and 3D optical data storage in particular[24]. The closed form has a conjugated path from one end of the molecule to the other, whereas the open form has not. This allows for the electronic communication between functional groups attached to the far ends of the diarylethene to be switched on and off using UV and visible light[24][25].

2.3.3 Absorbance Plots of Photochromic Molecules

Here we investigated the UV-Vis spectrum of the two photochromic molecules BTE and Diarylethene polymer. The photochromic properties of each AML were analyzed by spin-coating on a glass slide, irradiating with a Xenon Arc Lamp/ UV LED to make sure that it is in closed form B. And then at regular intervals, it is exposed to laser beam (HeNe) and conducted UV-Vis spectroscopy. Wavelength sources desired for *AMIL* are chosen based on the absorbance of AML corresponding to different wavelengths and availability. Absorbance *versus* time is plotted for two wavelengths λ_1 and λ_2, in particular to observe the time taken by the material for complete change in form. Also absorbances corresponding to repeated transition between the forms A and B are discussed.

The UV-Vis spectrum of Bithienylethene (BTE) is shown in Fig. 2.7. Measurements of this molecule are taken by spun-coating BTE of thickness ~600nm onto glass slide.

Absorbance corresponding to wavelengths ranging 250-900nm are obtained with the help of UV-Vis spectrometer. The sample is initially converted to closed form

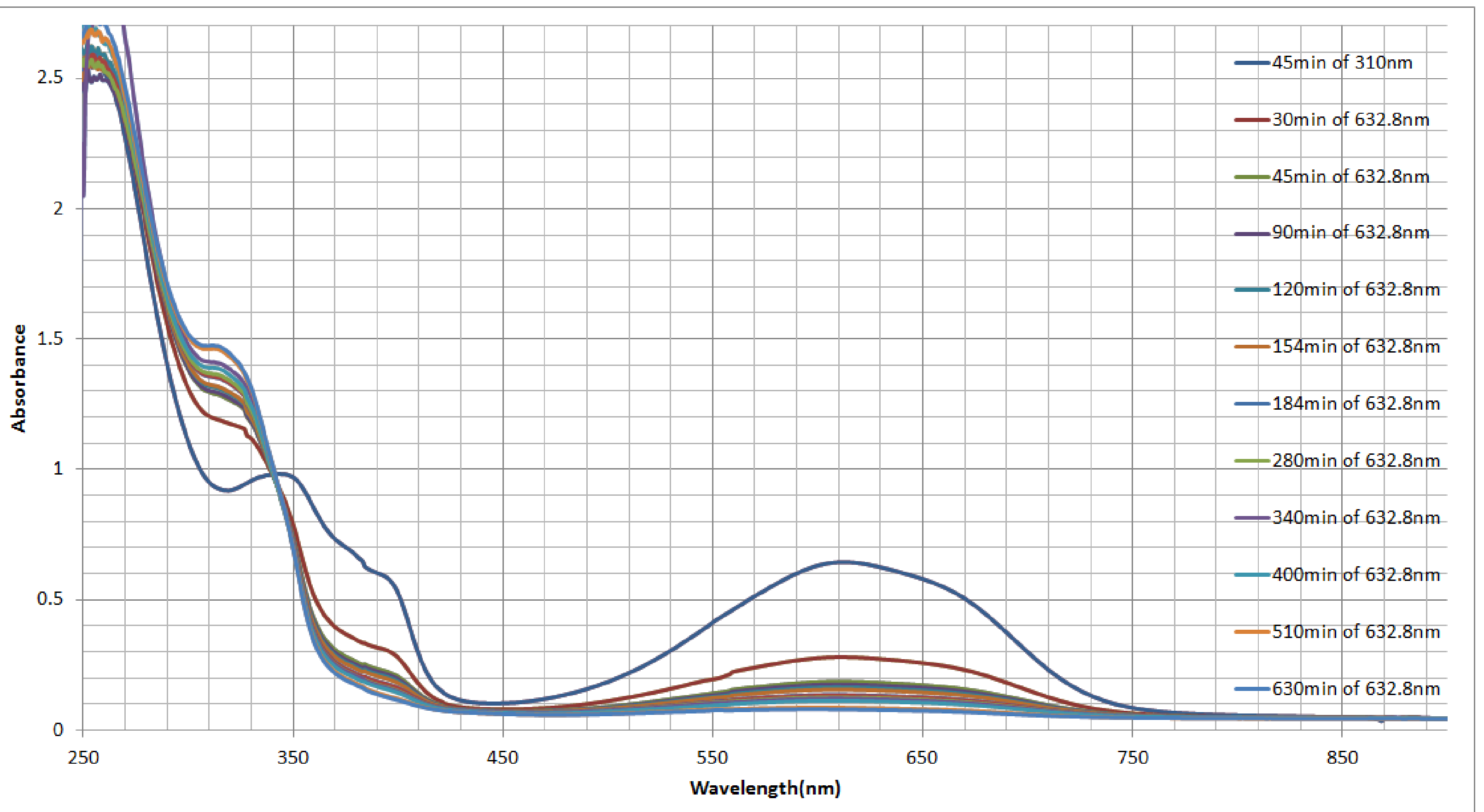

Figure 2.7: UV-Vis spectrum of Bithienylethene (BTE).

BTE in PMMA is spun-coated onto glass slide at a speed of 500rpm with a spinner such that thickness of the BTE layer is ~600nm. Sample is then exposed to UV beam having peak wavelength at 310nm for 45 minutes, to make sure it is in the closed form, whereas the intensity of this UV LED is 92.6uW/cm^2. UV-Vis spectroscopy is performed on this sample and also spectroscopy measurements are repeated at regular intervals of exposure to HeNe laser, of output wavelength 633nm. Intensity of this source is 13.79mW/cm^2.

by exposing it to UV. At regular intervals, it is exposed to HeNe laser whose output wavelength is 632.8nm until it is converted to open form, *i.e.,* no more change in the absorbance *w.r.t* time which is shown in Fig. 2.8. Spectrum in Fig. 2.7 corresponds to absorbance during this molecular transition from closed to open form.

The way this BTE molecule works as a photochromic material is described as follows. When the bond at the center between the two rings is open, the electrons of the two rings do not interact with each other much, creating two separate resonant cavities and an absorption peak at shorter wavelength. When the bond is close, the entire molecule forms a resonant cavity and creates another absorption peak at longer wavelength. The molecule was synthesized by Trisha L. Andrew, Chemist from Massachusetts Institute of Technology(MIT), USA. Its chemical structure during the two transitions is shown in Fig. 2.5. The peak of the open form is close to 300nm, and that of the closed form is close to 600nm. So, we used λ_1=310nm (UV LED had peak wavelength at 310nm) or 325nm from HeCd laser, and λ_2=633nm from a HeNe laser. This molecule was dissolved in a PMMA such that concentration ratio is 80% and 60mg/ml.

Absorbance of BTE corresponding to wavelengths λ_1=310nm and λ_2=633nm is shown in Fig. 2.8. When the molecule is in closed form, absorbance at λ_2 is 0.61828 and at λ_1 is 0.95025, thus acting as transparent to UV and absorbing most of the Red, creating a pathway to the wavelength that exposes resist and avoiding the wavelength that does not affect the resist. Then, we exposed this molecule to Red beam (HeNe laser), until the change in the absorbance is less than 1%. Final absorbance values of BTE layer after 1200 minutes of exposure to Red wavelength are at λ_2, absorbance is 0.0552 and at λ_1, absorbance of the layer is 1.36939, thus acting as transparent to Red and absorbing most of the UV, creating a pathway to the wavelength that does not expose the resist and blocking the wavelength that affects the resist.

The composition and UV-Vis spectrum measurements of the diarylethene polymer are shown in Figs. 2.9, 2.10 and 2.11. The way this molecule works is similar to BTE. The absorbance peaks for this molecule are also close to 300nm, in open form and close to 600nm, in closed form.

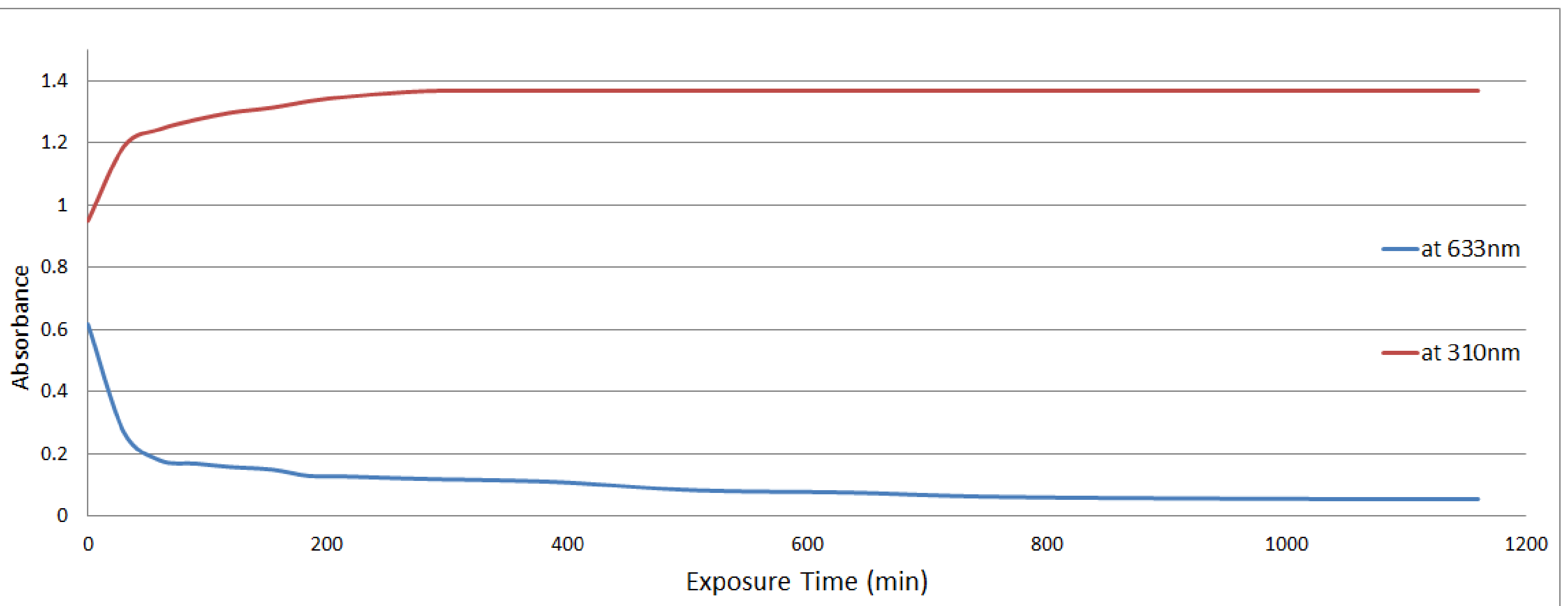

Figure 2.8: Absorbance of BTE *versus* time in minutes corresponding to wavelengths λ_1 and λ_2 during the transition from closed to open form.

These measurements are taken by exposing the spun-coated BTE layer to wavelength,λ_1=310nm (UV LED) for 45 minutes, intensity = 92.6uW/cm^2 and then at regular intervals to wavelength,λ_2=633nm (HeNe laser), intensity = 13.79mW/cm^2.

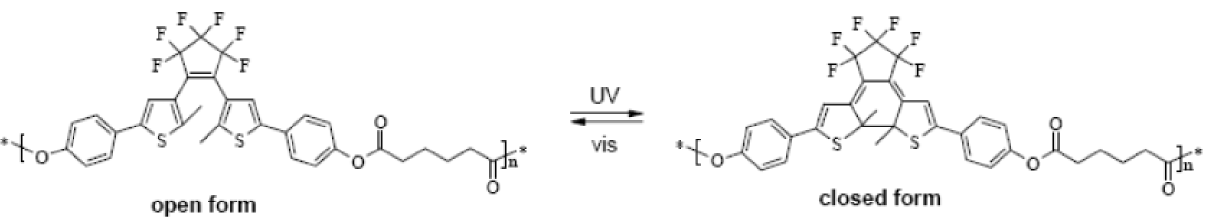

Figure 2.9: Composition of diarylethene polymer in open and closed forms.

The UV-Vis spectrum of Diarylethene polymer in chloroform of lesser concentration is shown in Fig. 2.10. Absorbance measurements on this molecule are taken by mixing the polymer in chloroform, such that concentration of the solution is 4mg/100ml, then spun-coating at 1000rpm onto a glass slide.

From Fig. 2.10, it is obvious that phototransitions at λ_1 and λ_2 are very narrow, which means that contrast in absorbance is not significant to observe the absorbance modulation. Low absolute absorbance at λ_1, results in low final image contrast in the resist.

Compared to Fig. 2.7 corresponding to absorbance of the BTE, the absorbance of the diarylethene film of thickness (250nm) is only 0.068, when the molecule is in closed form. With a 650nm thick film as shown in Fig. 2.11, the peak absorbance is about 1.0634 during its closed form state. Thus, 650nm thick diarylethene polymer film can provide enough image contrast to be recorded in the underlying photoresist but not with a thin diarylethene polymer film.

The UV-Vis spectrum of Diarylethene polymer in chloroform of higher concentration compared to the diluted one discussed earlier is shown in Fig. 2.11. Absorbance measurements on this molecule are taken by mixing the polymer in chloroform, such that concentration of the solution is 8.55mg/100ml, then spun-coated at 1000rpm onto a glass slide. After spun-coating, molecules are converted into closed form with Xenon-Arc lamp, short UV illumination λ_1 for 30 minutes. Intensity of this lamp at 310nm is 3.21mW/cm^2. Now for the reverse transition to open form, Diarylethene polymer is illuminated to HeNe laser beam of intensity 11.73mW/cm^2 for 120 minutes.

The UV-Vis spectrum of Bithienylethene (BTE) during its transitions from open to closed and closed to open forms, used in *Patterning via Optical Saturable Transformations (POST)*, is shown in Figs. 2.12 and 2.13 respectively. Measurements of this molecule are taken by thermally evaporating BTE of thickness ~100nm onto glass slide.

Just like UV-Vis measurements taken on BTE in *AMIL*, the sample (glass slide with evaporated BTE onto it) is initially illuminated with Short UV of intensity 3.061mW/cm^2 for 22 minutes. Then, the same sample is exposed to Red λ_2 to convert it into open form. UV-Vis measurements are taken during this process at different

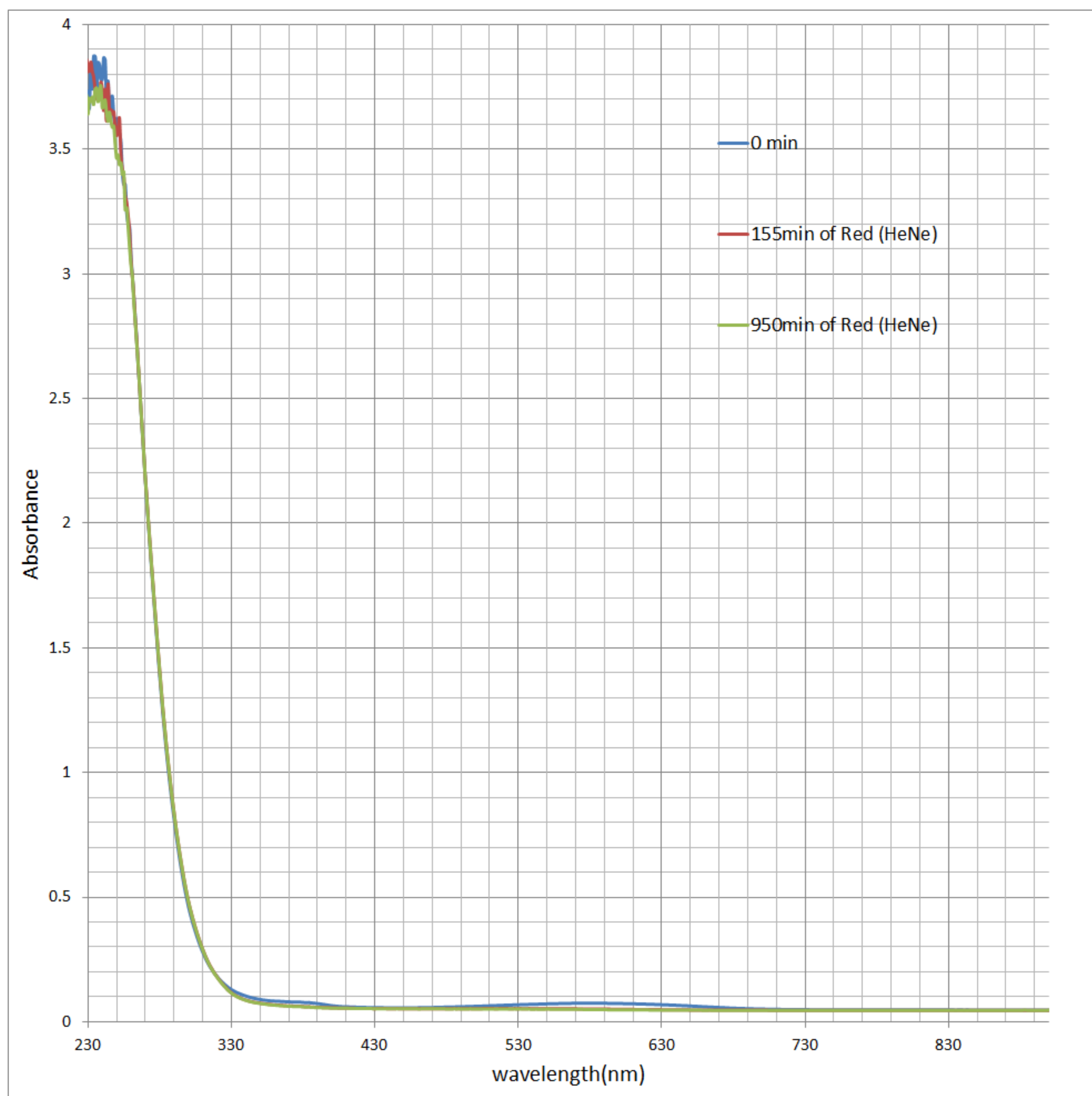

Figure 2.10: The UV-Vis spectrum of diluted diarylethene polymer.

Polymer in chloroform of concentration 4mg/100ml is spun-coated onto glass slide at a speed of 1000rpm with a spinner such that thickness of the layer is $\tilde{2}$50nm. Sample is then exposed to short UV light of Xenon-Arc lamp for 30 minutes, to make sure it is in the closed form, whereas the intensity of this UV light is 3.21mW/cm^2. UV-Vis spectroscopy is performed on this sample and also spectroscopy measurements are repeated upon exposure to HeNe laser, output wavelength 633nm. Intensity of this source is 10.99mW/cm^2.

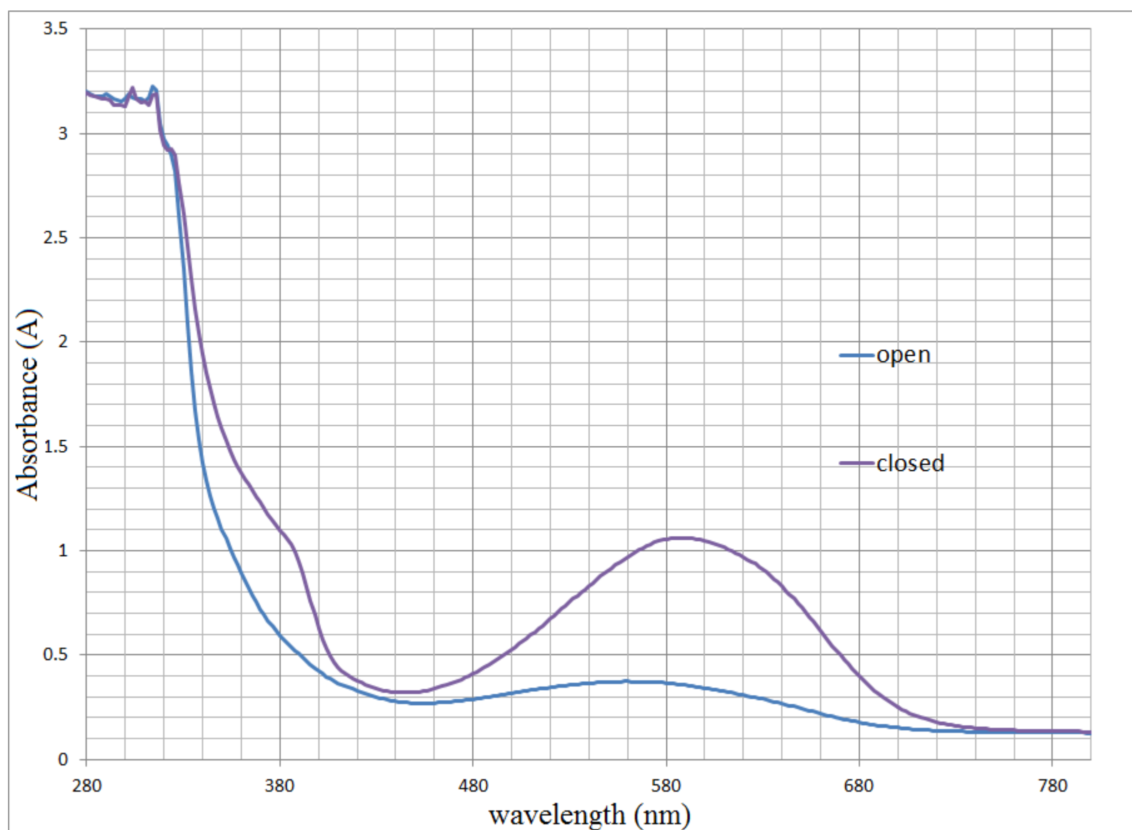

Figure 2.11: The UV-Vis spectrum of diarylethene molecules used for AML.

The diarylethene molecules are again dissolved in chloroform but this time concentration is around 8.55mg/ml, to increase the signal to noise ratio for the UV-Vis measurement. It can be seen that the diarylethene is absorbing when it is in closed form and less absorbing when it is in open form. λ_1=310nm illumination was applied to for the transition from open form to closed form, and λ_1=633nm illumination was applied for the reverse transition.

intervals as shown in Fig. 2.12. Now the sample is again illuminated with Short UV of intensity 2.8765mW/cm^2 at 310nm to convert it into closed form. UV-Vis measurements are repeated at different intervals as shown in Fig. 2.13. Significant change in absorbances in the desired manner are occurring at the wavelengths 330nm and 600nm. Based on the sources available we used Short UV/ UV LED having peak wavelength at 310nm and He-Ne laser having an output of wavelength 632.8 nm (633nm).

During the transition of BTE between its forms, change in absorbances over a period of time are plotted at the wavelengths 310nm and 633nm. In Fig. 2.14, (a)

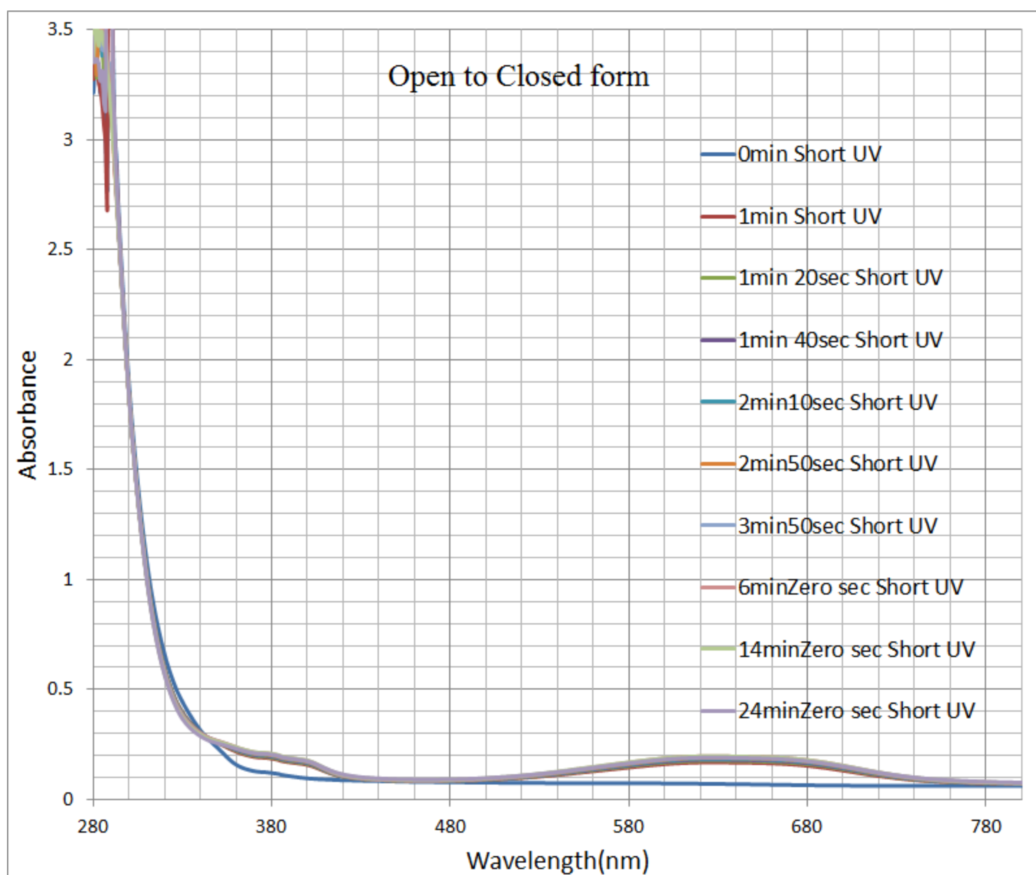

Figure 2.12: UV-Vis spectrum of BTE used in *POST* during its transition from open to closed form.

Upon thermal evaporation of BTE onto glass slide, the sample is exposed to Short UV from Xenon-Arc lamp of intensity 2.8765mW/cm^2 at 310nm. The above processes are repeated until the molecule is completely converted to closed form, which is known from a much smaller percentage change in absorbance.

and (b) correspond to absorbances at 633nm and 310nm during transition of BTE from open to close form, whereas (c) and (d) also correspond to absorbances at 633nm and 310nm but during the reverse transition of BTE to open form. Here it is obvious that within a few minutes we can convert the BTE from open to close form but for converting back into open form it has to be exposed to λ_2=633nm of intensity 9.469mW/cm^2 for at least 2 hours to make sure that the molecule completely changes its form. For this reason, while doing a double exposure with the help of nanoposition piezoelectric stage (will provide precise control over the linewidth of the periodic grating which is directly proportional to the extent the stage is moved) between the

exposures, leave the sample under λ_2=633nm for few hours by turning OFF the UV power supply (no simultaneous UV illumination during molecular transition). So that BTE is completed converted back to open form. Once BTE is converted, simultaneous second exposure with λ_2=633nm and λ_1=310nm is repeated.

Absorbance of BTE at the wavelength λ_2=633nm over a period of time between its repetitive transitions open to close and close to open forms by exposing the sample to short UV λ_1 of intensity 2.629mW/cm^2 at 310nm and Red λ_2=633nm of intensity 9.469mW/cm^2, respectively, is observed and is plotted as shown in Fig. 2.15. This variation in absorbance is also an important parameter that should be considered while doing multiple exposures (especially more than two exposures), because based on the requirements for the latest design techniques, having complicated periodic structures we might need to do more than two exposures on the same sample without removing or adding photochromic molecules. Then, exposure doses should be

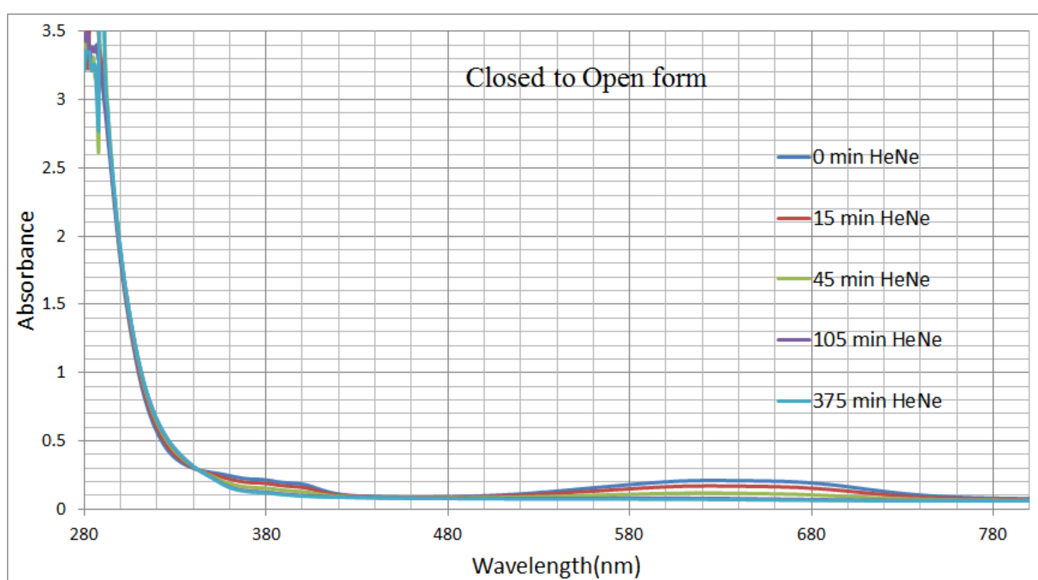

Figure 2.13: UV-Vis spectrum of BTE used in *POST* during its transition from closed to open form.
UV-Vis spectroscopy is performed on this sample at regular intervals of exposure to HeNe laser, of output wavelength 633nm in the same way as we did spectroscopy measurements during the transition from open to closed form . Intensity of this Red beam while illuminating the sample is 13.79mW/cm^2.

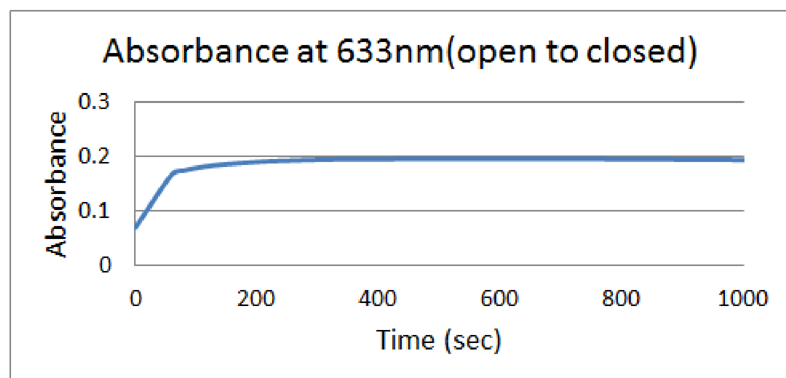

(a)

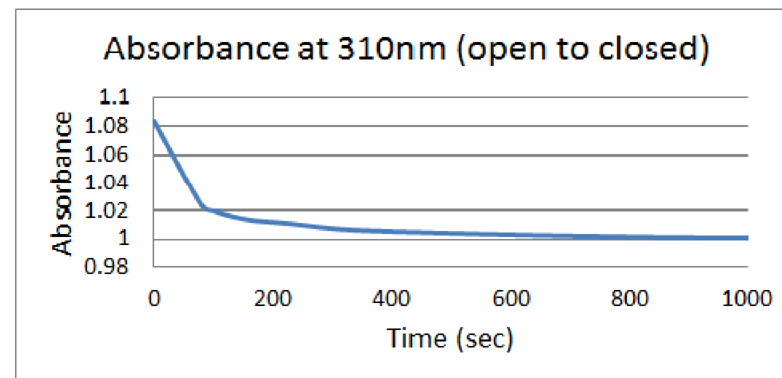

(b)

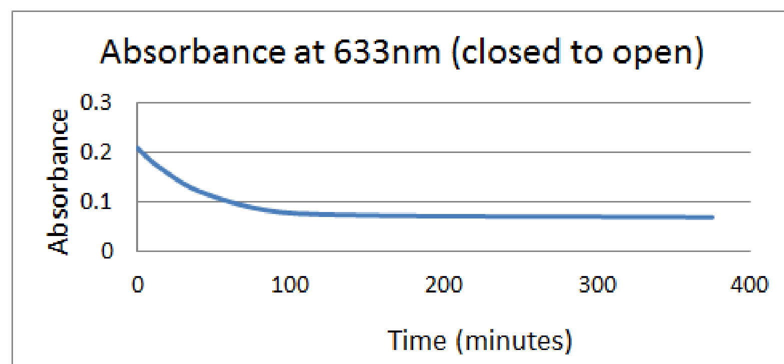

(c)

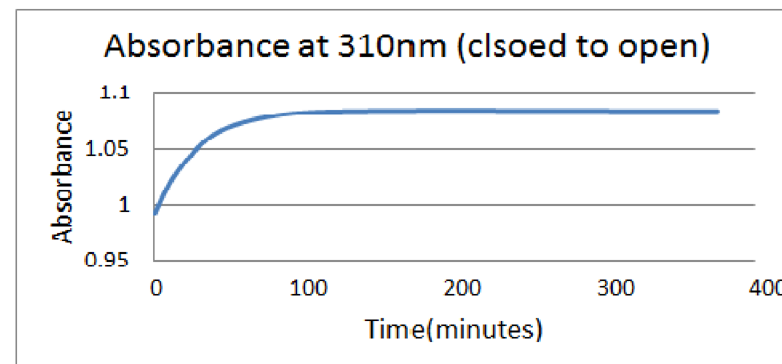

(d)

Figure 2.14: Absorbance of BTE at 310 nm and 633 nm during its transition from open-close and close-open forms.

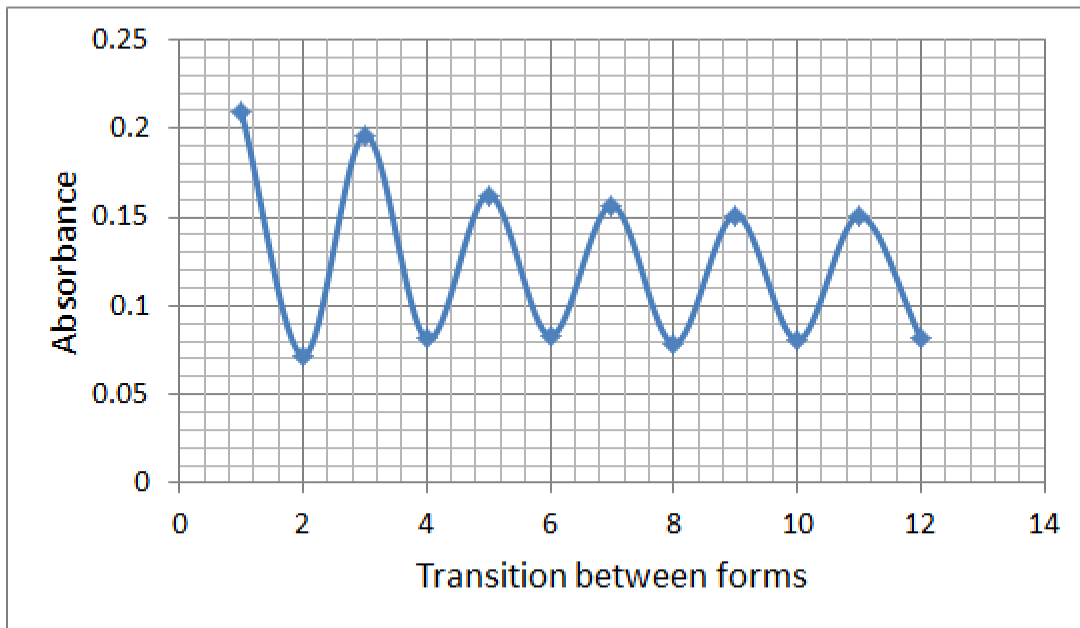

Figure 2.15: Absorbance of BTE at λ_2=633nm during its repetitive transitions between open-close forms.

adjusted based on the absorbance value of the BTE. As the number of repetitive exposures increases on a sample without altering the BTE layer, limitation of this technique increases due to decrease in absorption contrast of photochromic molecules at different wavelengths *esp.* at λ_1 and λ_2 during its molecular state, i.e., open and close forms.

2.4 MATLAB Simulations - Power Reflectivity

Power reflectivities from the lower layers in the stack of layers with irradiation to two wavelengths were investigated in this part. It is found out that higher power reflectivity will cause nonuniformity in the lithography step, *esp.* due to this higher back reflections. Power reflectivity between the photoresist and Anti-Reflection Coating (ARC)/ Silicon interface is simulated in MATLAB and presented various results which are based upon optical constant of all the layers in the stack, their thickness's accurate resist layer thickness in particular, angle of incidence, polarization and wavelength source. Where the greatest percentage of reflectivity is from the Silicon which is at the bottom of all the layers in the stack, in the *Absorbace Modulation Interferometric*

Lithography AMIL technique is the root cause for nonuniformity in the resist layer which we observed earlier.

The MATLAB code used for this power reflectivity simulation creates a GUI to display 1D/2D reflectivity measurements based on the number of variables. These simulations are done considering the exact individual layer thicknesses of the stack used so far, angle of incidences (angles at which Red and UV beams are incident onto Si sample in a practical set-up are considering while doing simulations than just taking somme random values). Both 1D and 2D simulation results of this code are explained in brief in the following paragraphs.

Power reflectivity 2D simulations corresponding to wavelengths λ_1=325nm and λ_2=633nm at two different angles, one original angle of incidence and the other (90° - angle of incidence) for the thin or thicker resist and Anti-Reflection coating are shown in Fig. 2.16. All these simulations and also the ones to be discussed later in this section are performed only in TE polarization mode.

TM polarization mode corresponding to all the presented simulations (figures corresponding to this mode are not presented), no significant variation in power reflectivity values *w.r.t* thickness of the layer is observed. In Fig. 2.16, (a) and (b) correspond to wavelength λ_1=325nm, where the angle of incidence is 20° and 80°, respectively, and (c) and (d) correspond to λ_2=633nm, where the angle of incidence is 27° and 63°, respectively. From these figures, it is observed that power reflectivity value is not varying much *w.r.t* resist layer thickness whereas it is more sensitive to only ARC layer thickness. Also comparing ARC layer thickness among the simulations corresponding to λ_1 and λ_2, to make the percentage of power reflectivity the $<5\%$ ARC layer should be much thicker for λ_2 than for λ_1. Again it does not really matter how much power is reflected corresponding to λ_2 because it is not going to affect the resist. Only λ_1 will expose the resist and also the more the power of this wavelength reflected corresponds to the more the nonuniformity seen on the photoresist. For this reason based on the simulation corresponding to λ_1, ARC layer thickness is chosen for a particular photoresist layer thickness.

Figs. 2.17(a) and (b) correspond to 1D simulations of power reflectivity with antireflection coating as a variable in the stack with Shipley S1813 photoresist layer of

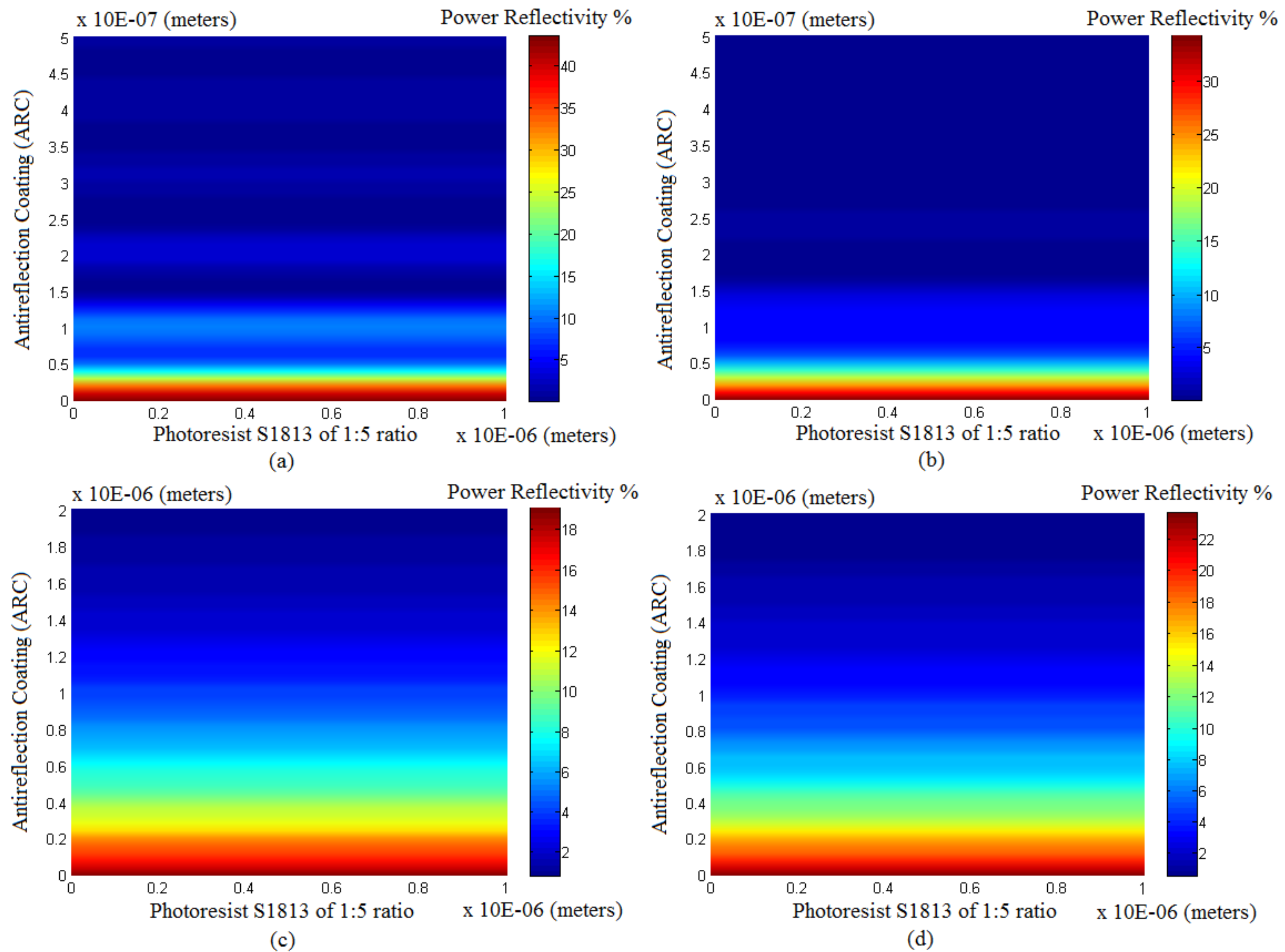

Figure 2.16: 2D MATLAB simulation of power reflectivity at the interface of antireflection coating and photoresist layer

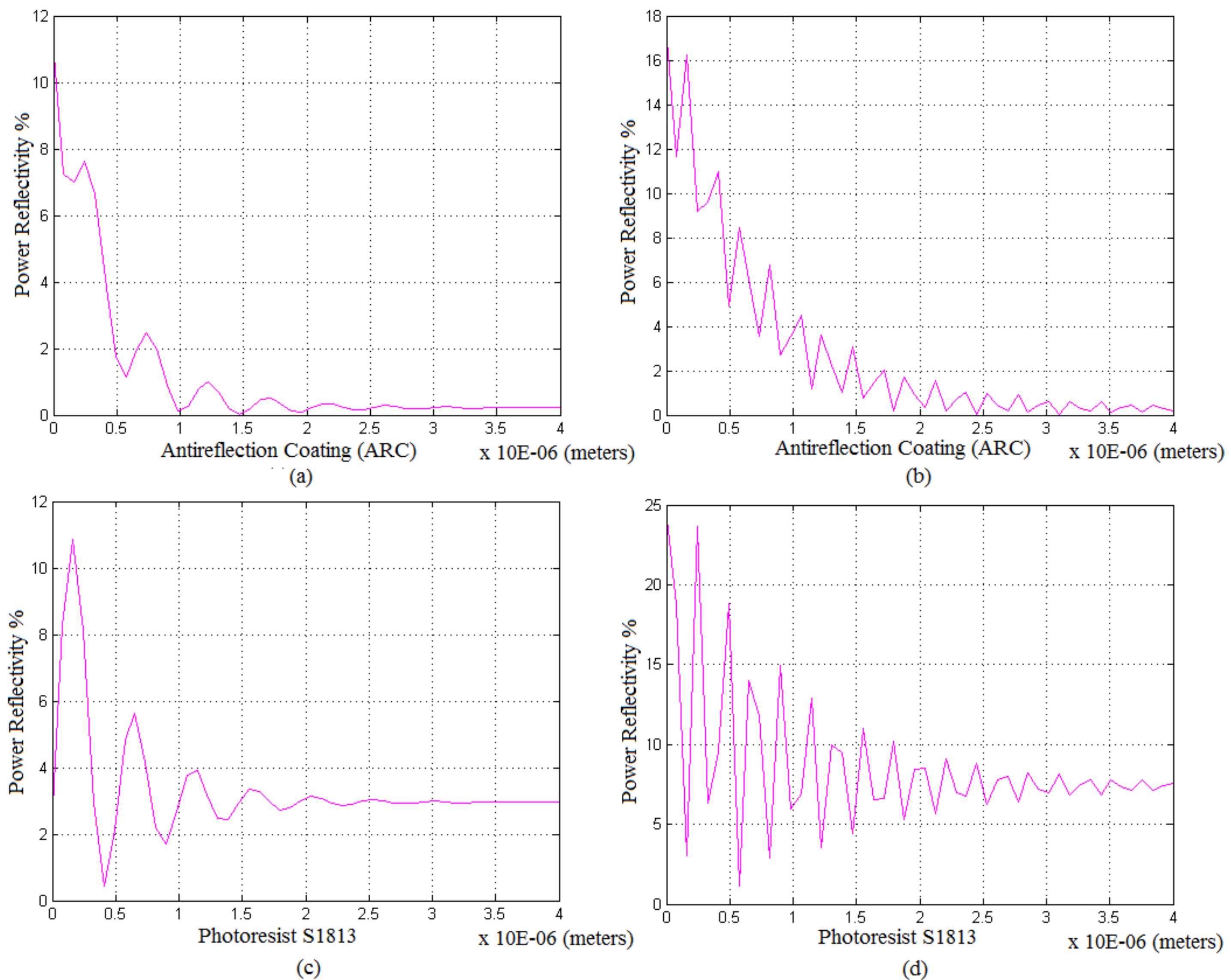

Figure 2.17: 1D MATLAB simulation of power reflectivity with either antireflection coating or photoresist layer thicknesses as a variable in the stack.

thick 1.2μm, Poly-Vinyl alcohol (PVA) of 10nm and BTE of 686nm for λ_1=310nm and λ_2=633nm, respectively, whereas in Figs. 2.17(c) and (d), photoresist layer thickness is the variable in a stack with PVA and BTE of same thicknesses discussed earlier and moreover without antireflection coating at all. From the simulations presented in Fig. 2.17, we can obtain the required antireflection coating layer thickness to minimize the back reflections at photoresist-antireflection coating layers interface and also minimum photoresist layer needed to avoid maximum power reflections from the Silicon. Based on these simulations, *AMIL* experiments were performed and are explained in brief in Chapter 3.

Two-dimensional MATLAB simulations corresponding to *POST* samples are seen in Figs. 2.18 and 2.19. In these figures, (a), (b) and (c) correspond to stack of BTE, Platinum and ARC layer top-bottom architecture, angle of incidence is 31° but BTE layer thickness is 15nm, 50nm and 80nm, respectively. From Figs. 2.18 and 2.19, it can be concluded that for the given angle of incidence, irrespective of BTE layer thickness to have the power reflectivity $<1\%$, the platinum layer should be $\leq$5nm and also the ARC layer should be of 118 - 130nm.

Even with minimum power reflectivity calculations, we still could be able to see some roughness in the photoresist during the *AMIL* exposures. Now, two other parameters which are assumed to be the reason for this are

(i) Blocking/protecting layer polyvinyl alcohol (PVA); it is dubious that PVA is not really protecting the resist from BTE.

(ii) Nonuniformity of photochromic molecules within the BTE layer spun-coated. To check this confocal microscopy images are obtained.

More about these assumptions are explained in Chapter 3 along with *AMIL* experimental results.

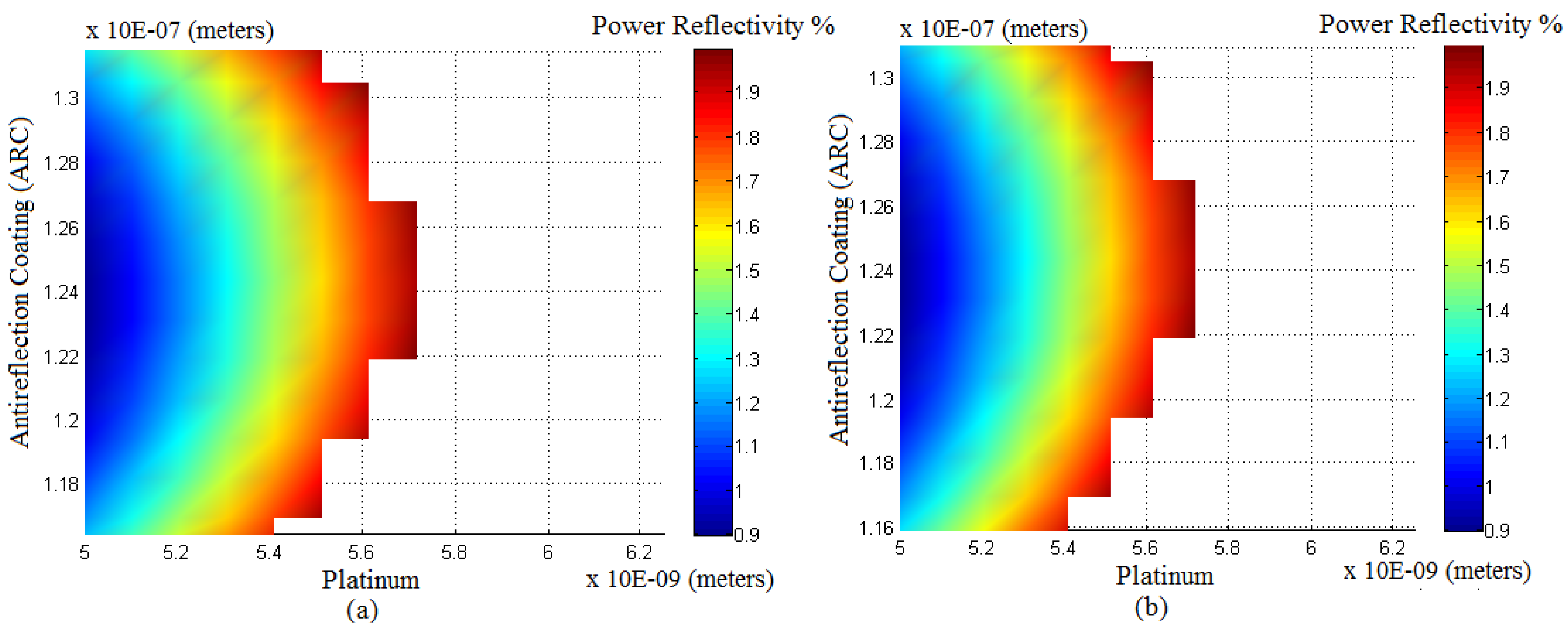

Figure 2.18: 2D MATLAB simulation of power reflectivity with antireflection coating and thickness of the Platinum layer as variables

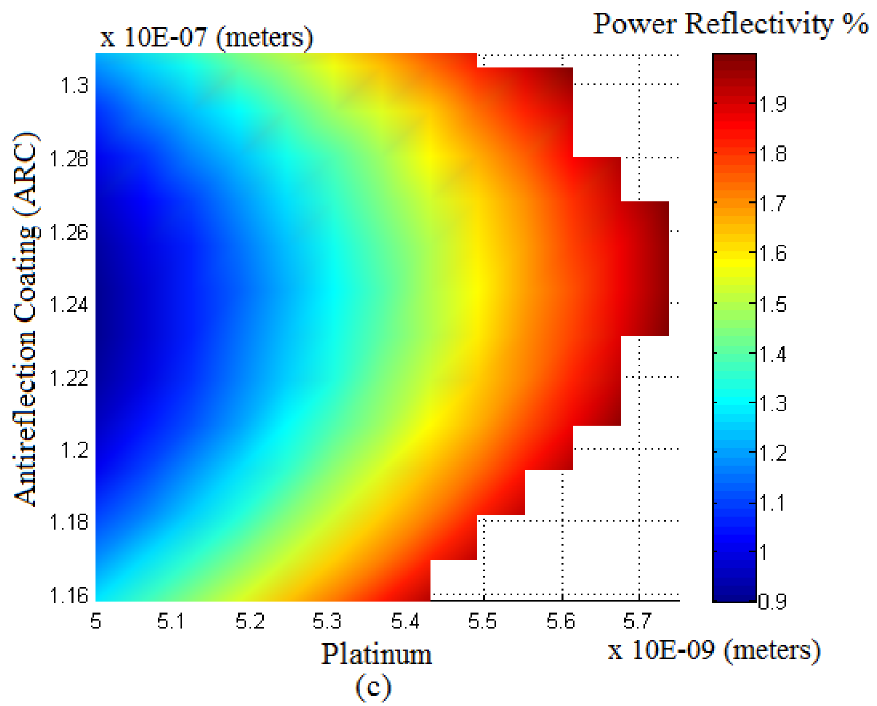

(c)

Figure 2.18: continued

CHAPTER 3

ABSORBANCE MODULATION INTERFEROMETRIC-LITHOGRAPHY (AMIL)

Absorbance Modulation Interferometric-Lithography (AMIL) is a novel optical lithography technique that has the ability to overcome the diffraction barrier.

3.1 Experimental Setup

Canonical experimental setup of the proposed research, *Absorbance Modulation Interferometric-Lithography (AMIL)*, based on the Lloyd's mirror interferometer system is shown in Fig. 3.1. *AMIL* requires two different wavelengths, so a special optical system is constructed [26]. One of the first systems that was built is an interference system that will incorporate two wavelengths (λ_2=632.8nm, λ_1 = 325nm) by He-Ne Laser and UV lamp, respectively. The source of λ_1 may be inexpensive UV LEDs or UV lamps.

Initially experiments were performed using UV lamp which had short and long UV range selections. But now, we are using UV LED which had wavelength peak at 310nm (i.e., λ_1 = 310nm) due to power and other optical issues, whereas, λ_2 is He-Ne laser in both cases.

In Fig. 3.2, experimental setup of AMIL is shown. The only modifications in this figure when compared to Fig. 3.1 are that the UV source is LED instead of UV lamp and an extra optics (spatial filter) to alter the beam from the LED. We even did some exposures using HeCd Laser as a replacement for the UV LED/UV lamp not shown in either of the figures. To make the system very economical and reliable, we started using UV LED. The only limitation of equipping UV LED is

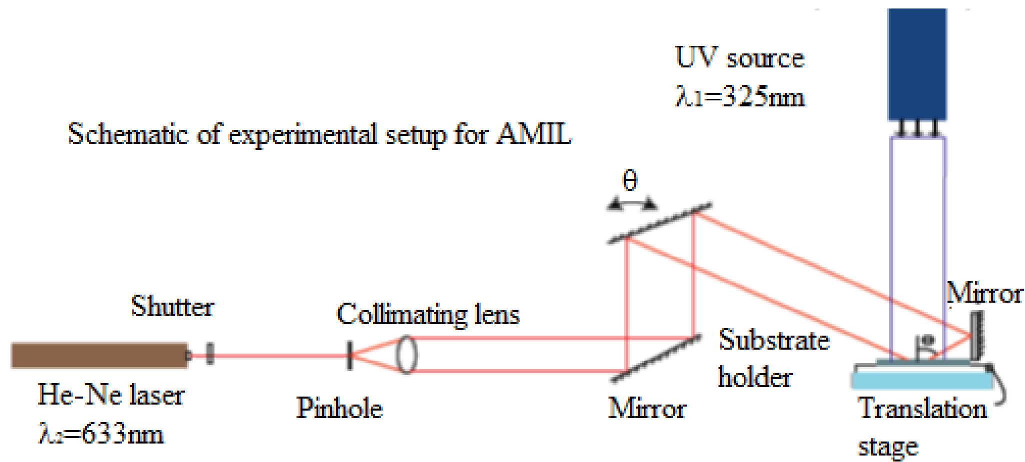

Figure 3.1: Schematic of AMIL approach

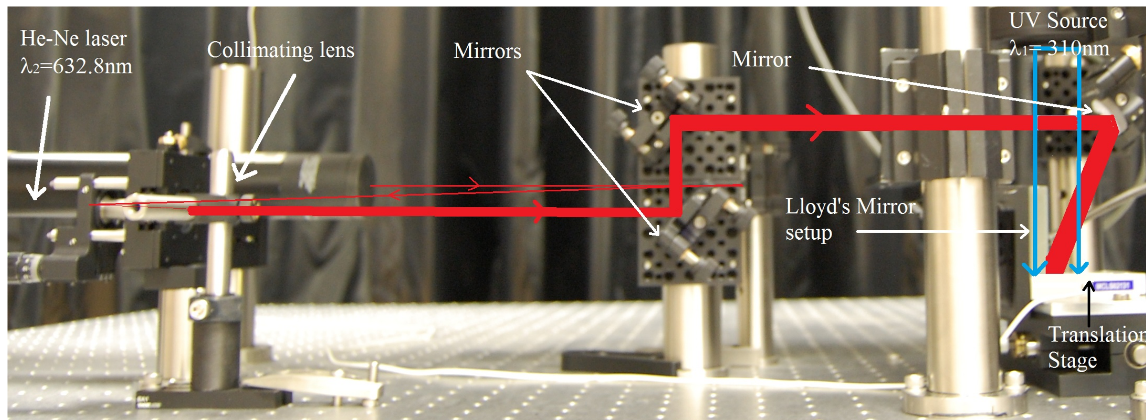

Figure 3.2: Recent AMIL experimental setup with piezo-controlled nanoprecision stage controllable by LabVIEW

power constraints; intensity is only an order of a few μW/cm^2 when compared to the other two sources used in this research.

3.2 Layers in the Sample Stack

The sample on which *AMIL* exposures are done had a stack of four layers on top of each starting with antireflection coating of ~200nm to 1.5μm, thickness chosen is based on the type of resist and its thickness through MATLAB simulations explained in Chapter 2, positive resist; Shipley 1813 positive photo resist (thickness varies) is the most common resist used in the sample preparation for the exposures discussed

in this chapter, Poly Vinyl Alcohol (8-10nm) to prevent photochromic molecules from diffusing into photo resist, *i.e.,* it acts as a blocking layer in between photoresist and photochromic molecules layer which can be easily removed with DI water either by sonication or by just dipping it in the DI water for 30 seconds, photochromic molecule Bithienylethene (BTE) in PMMA spun-coated such that the thickness is of ∼700nm. A schematic of this kind of sample with all the stack of layers is shown in Fig. 3.3. Other kinds of resists tested with *AMIL* include chemically amplified resist TDUR, Negative resist - SU8 & AZnLOF 2020, etc. Different kinds of PVA ranging from the one with different molecular weight to chemically amplified ones are used in the process of getting rid off roughness, for better *AMIL* exposures. More details about this can be found in section 3.4. We tried to replace the blocking layer (PVA) with a few metals, such as Au, Cu, *etc.* But it turned out be difficult to get rid of metals easily and also selection of material is limited because of exposing the resist while depositing any other layer that can act as a blocking layer between the resist and photochromic molecules.

3.3 Sample Preparation

All the layers in the sample used for AMIL are prepared by spun-coating at different speeds on a spinner. Prior to spun-coating any of these layers, initially each one of them is intensively calibrated in terms of thickness and roughness. We even tried to replace PVA with some other layer and thermally evaporate BTE

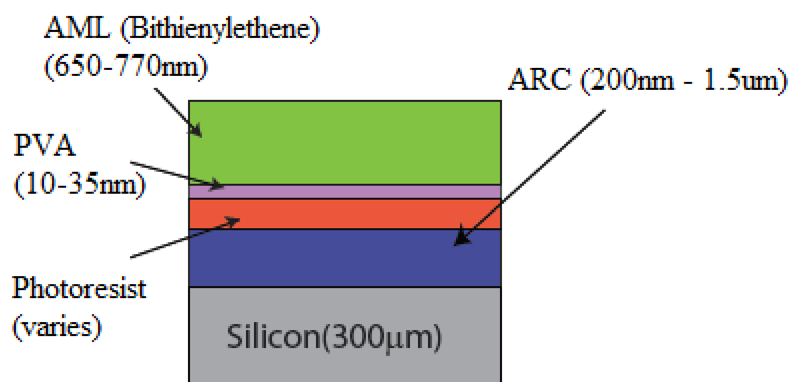

Figure 3.3: Schematic of AMIL sample with all the layers in the stack

onto the sample. But no significant improvement was observed with that and also relatively less absorbance contrast with BTE from UV-Vis spectrum measurements, so we continued with spun-coating instead of thermal evaporation. For the later experiments discussed in this chapter, ARC is not included in the stack. Instead we used a thicker resist. Some exposures are tried on the samples with very thin resist also without ARC for the sake of lower exposure doses when compared to thicker resist. Respective steps in preparing the most recent sample are mentioned in the last subsections.

3.3.1 Antireflection Coating (ARC)

An antireflection coating is a type of optical coating applied to the surface of the sample to reduce back reflection from the Silicon surface in our research. Apart from this, people use this layer for many other applications.

Until recent exposures, Az Barli II 90 is spun-coated at 2000rpm onto Si thus forming a ∼200nm of layer, acting as an antireflection layer. Later based on the thickness requirement, the previous step is repeated 7-8 times on top of each other by spun-coating the material at 1000rpm thus forming a film of $\sim 1.2\mu$m. In the most recent exposures the stack does not have the ARC layer, which is replaced with thicker resist.

3.3.2 Photoresist

Photoresist is a type of light sensitive material upon exposure to light due to absorption at UV and shorter wavelengths causing electronic transition[27]/carbon double-bond chromophores[28]. It becomes more soluble in the portions where it is exposed and remains insoluble in the areas where it is unexposed to UV with a solution (photoresist developer). Photoresists can also be exposed by electron beams[29]. The primary aim of this project is the photoresist onto which a period pattern has to be created. The most commonly used photoresist in *AMIL* is Shipley S1813. Shipley S1813 is a positive photoresist, i.e., upon exposure to UV wavelength, the material becomes soluble in the developer , or else it is insoluble. So, during the *AMIL* exposures, portions down the optical apertures to BTE that are exposed to

UV are washed away upon immersing the sample after the desired exposures in a developer solution and those portions that are not beneath the apertures of BTE are not exposed to UV because of the blocking nature of the absorbance modulation layer to λ_2, insoluble in developer solution, thus creating a periodic pattern due to apertures created with Interferometry using the Absorbance Modulation technique.

Here the photoresist is spun-coated at different spin speeds based on the thickness requirements, with a spinner and then prebaked to cure the photoresist. Before prebake, photoresist still has much solvent. This prebake may be done in several ways especially depending on the type of resist. In some cases, postbake (not to be confused with postexposure bake that comes before development)[30], i.e., baking at higher temperatures (usually 120-150°C) will cross-link the resin polymer in the photoresist, thus making the image more thermally stable, is performed, whereas postexposure bake (PEB), which is baking after the exposure but before developing the sample, may also be performed before the transferring the pattern onto Silicon.

Photoresist Shipley S1813 is diluted further in Thinner P to create films of only few tens of nanometers. Different resist used in this project are Shipley S1813 positive photoresist and its diluted forms, chemically amplified resist TDUR (by Tokyo Ohka Kogyo Co., Ltd.), negative resists SU-8 series and AZ nLOF 2020.

Resist is spun-coated on top of ARC layer (if it is present)/Silicon substrate with a spinner and then it is prebaked at 115°C for 2 minutes. For thinner S1813 resist of ratio 1:11, it is spun-coated with a spinner and then the sample is prebaked at 115°C for 15 minutes. The prebaking temperature of this particular resist with hotplate should not exceed 120°C.

3.3.3 Polyvinyl Alcohol (PVA)

Polyvinyl alcohol is a water-soluble synthetic polymer having excellent film forming, emulsifying and adhesive properties. In this project, this PVA is used as a protective/blocking layer between the photoresist and photochromic molecules. Earlier PVA of different molecular weights from Sigma-Aldrich mixed in DI water is used as a blocking layer, but recently, in most of the exposures a chemically amplified PVA is used. This PVA is spun-coated on spinner such that the thickness is ∼10nm. The sole

purpose of this layer to protect the resist from the top layers, which means that the layer thickness should be as minimal as possible such that there are minimal effects due to contrast between the layers. At the same time it should be thick enough to avoid diffusing molecules from the top layers. More about this is discussed in section 3.4.

Chemically amplified PVA is spun-coated on top of the resist with a spinner by filtering the solution with 0.45μm filter, glass syringe. Then it is baked on a hotplate at 80°C for 90sec. Earlier we tried doing desiccation and also overnight drying of the layer before putting any layer on top of this.

3.3.4 Photochromic Molecules

Photochromic molecules switch reversibly between two stable isomers when irradiated with light. The diarylethene polymer is a photochromic molecule discussed in Chapter 2 that can exist either as the colorless open form A, or as closed form B, which has a dark blue color. When the bond at the center between the two rings is open, the electrons of the two rings do not interact with each other much, creating two separate resonant cavities and an absorption peak at shorter wavelength. When the bond is close, the entire molecule forms a resonant cavity and creates another absorption peak at longer wavelength. Similar functionality with BTE as well. UV-Vis measurements that describe the absorbance of the photochormic molecules BTE and Diarylethene polymer are described in Chapter 2.

Bithienylethene (BTE) in Poly(methyl methacrylate) (PMMA) 80%/60mg/ml is spun-coated on top of PVA with a spinner by filtering the solution with 0.2μm filter, glass syringe. It is observed that film quality becomes even better if it is thermally annealed. Then, after spun-coating the BTE, the sample is baked in an oven at 110°C for 1 hour. For the initial exposures, we did not do the thermal annealing step of BTE, which might be the reason behind the initial roughness observed on photoresist with *AMIL* exposures. Similarly, Diarylethene polymer 8.55mg/ml of Chloroform is spun-coated on top of PVA with a spinner. Even these samples are thermally annealed before using them for *AMIL* exposures.

3.4 PVA Roughness Analysis

As discussed earlier in this chapter, the sole purpose of the PVA layer is to protect the resist from its top layers. In this case it is a spun-coated photochromic layer. PVAs of a different molecular weight and also of different concentrations are tried to form a thin protective layer. From Fig. 3.4, it is evident that even though spun-coating PVA (high molecular weight: 12500)of different concentrations is not forming a uniform film in most cases. This could be a strong reason behind the roughness seen on the photoresist with *AMIL* exposures that used PVA of lesser concentration/thin layer thickness, because if PVA layer formed upon spun-coating is not uniform, holes in the layer mean that it is not completely protecting the resist from photochromic molecules which attack the resist badly through those gaps.

In Fig. 3.4, (a) and (b) correspond to PVA of concentration 0.4g/100ml which is spun-coated onto a sample with a spinner at 1000rpm and then the sample is left for an overnight dry / dessicated the sample, respectively. Fig. 3.4 (c) and (d) correspond to concentration 1g/100ml and spun-coated at 6000rpm, then overnight dried / dessicated, respectively. Fig. 3.4 (e) and (f) correspond to the same concentration 1g/100ml but this time it is spun-coated at 2000rpm, then overnight dried / dessicated, respectively. Fig. 3.4 (g) and (h) correspond to concentration 2g/100ml and spun-coated at 6000rpm, then overnight dried / dessicated, respectively. Fig. 3.4 (i) and (j) correspond to the same concentration 2g/100ml but are spun-coated at 2000rpm, then overnight dried / dessicated, respectively.

From the analysis, it is found that only one blocking layer, which is formed by PVA (molecular weight: 12500), of concentration 2g/100ml and then spun-coated at 2000rpm, is forming a uniform layer or layer without any openings. Thus for all the *AMIL* exposures after this analysis, the PVA layer is formed by spun-coating the material with these specifications, i.e., PVA of concentration 2g/100ml, spin-coating at 2000rpm. Using the same concentrated PVA, the solution can be spun-coated at even lower RPM to form a thicker film. But the PVA layer should be as thin as possible because of the contrast issue between the photoresist layer and photochromic molecules layer. Then the significant improvement in the exposure grating is observed.

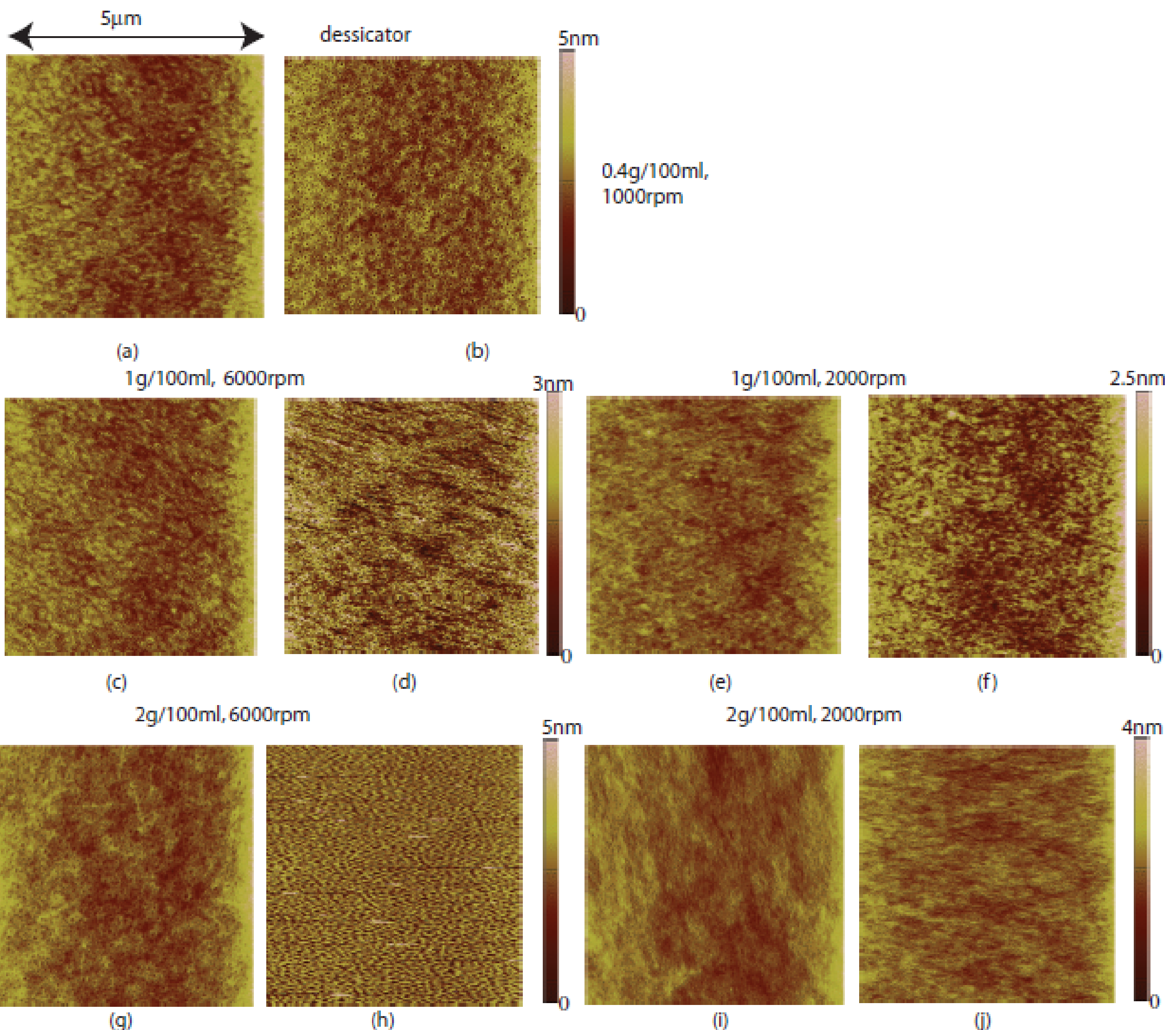

Figure 3.4: AFM images of PVA layer corresponding to different concentrations and ways of curing

Later we started using chemically amplified PVA, to form a layer of 10nm and also moreover it is uniform at this thickness and does not have any holes.

Since PVA is water-soluble, both the layers PVA and BTE/Diarylethene polymer are easily removed by doing sonication in DI water. If it is not water soluble, the top layer (BTE/Diarylethene polymer) has to be removed separately with its respective solvent and then PVA. Since PVA has a glass transition temperature at 80°C, the sample after putting PVA by spun-coating is baked at this temperature and for doing thermal annealing of BTE/Polymer, the sample is baked in an oven at higher temperature, say 110°C, instead of a hot plate, whereas glass transition temperature of PMMA, which is a solvent for BTE, is 95-106°C.

3.5 Experimental Results

AMIL experiments and results are discussed in this section. All the results are categorized under two subsections, one set having BTE as *Absorbance Modulation Layer (AML)* and the other having Diarylethene polymer as *AML*. Thickness of the antireflection coating, photoresist and PVA are varied from sample to sample in most cases. Limitations are due to exposure dose, experimental setup, etc.

3.5.1 BTE as Absorbance Modulation Layer

In this subsection, all the samples had BTE as an AML in the stack. Thus, the stack is a composition of ARC, photoresist (Shipley S1813/chemically amplified resist; TDUR), PVA and BTE. In Fig. 3.5, (a) and (b) correspond to Shipley S1813 resist of thickness $\sim$1.2μm, Source wavelengths, λ_1 = 325nm and λ_2 = 633nm. Intensity of λ_2 is 4.98mW/cm^2 and of λ_1 is 462.96μW/cm^2, whereas doses are 70 and 255 minutes, respectively. Fig. 3.5 (c) and (d) also correspond to S1813 resist but of thickness $\sim$1.2μm. Now λ_1 = 310nm and λ_2 = 633nm. Intensity of λ_1 is 4.815μW/cm^2, of λ_2 is 2.9mW/cm^2. Doses of these two exposures are 290 and 180 minutes, respectively. Finally, Fig. 3.5 (e) and (f) correspond to chemically amplified resist TDUR of thickness 100nm. Again, $\lambda_1 = 325$nm and $\lambda_2 = 633$nm with intensities of λ_1 is 0.37μW/cm^2, of λ_2 is 4.94mW/cm^2. So, now doses are 25 and 124 minutes, respectively.

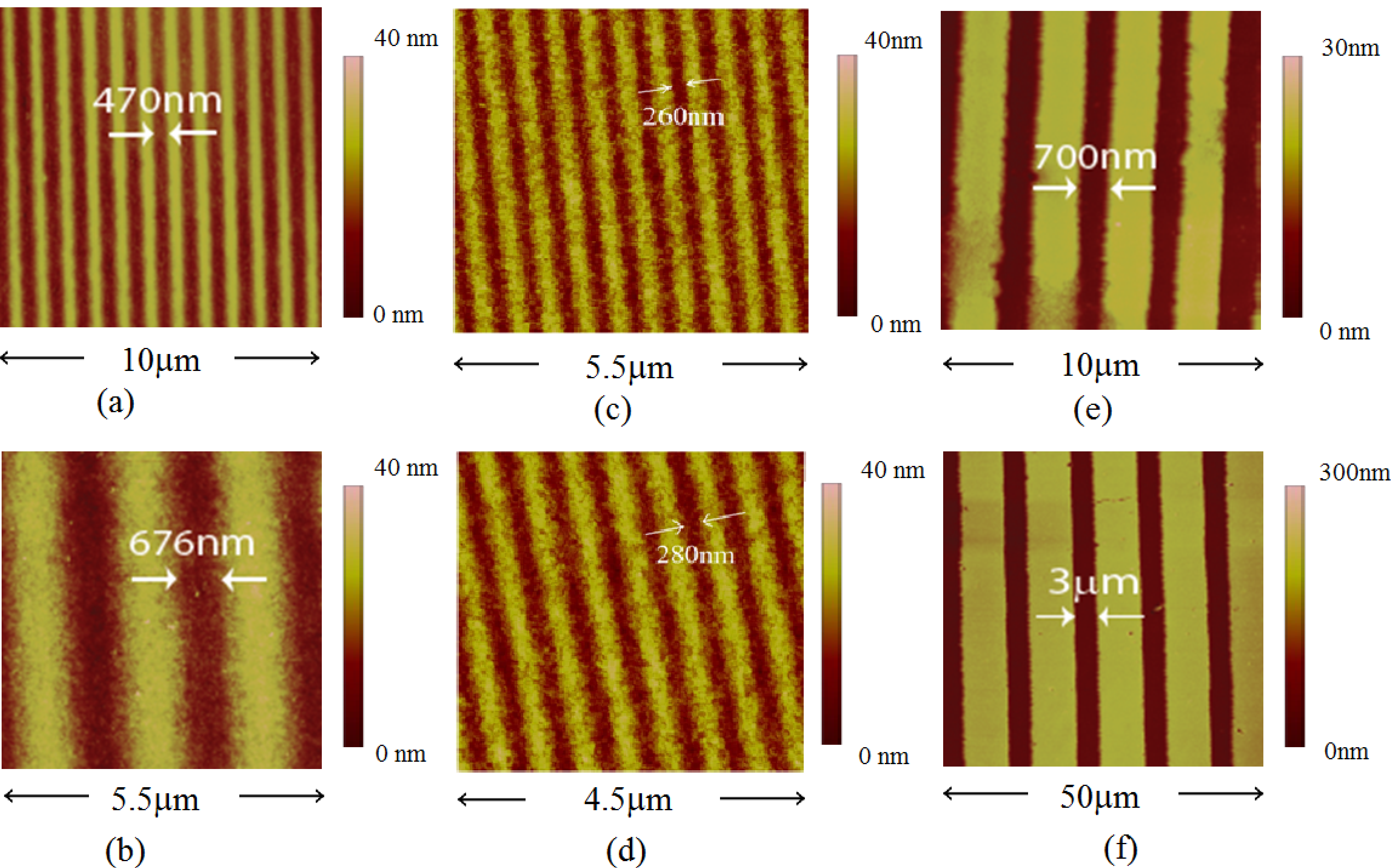

Figure 3.5: AFM images of different *AMIL* exposures with BTE as AML

Even though grating is observed, it is not significant in terms of exceeding the diffraction limit/capable of doing multiple exposures. In an attempt to decrease linewidth of the periodic grating, grating became even worse. The primary reason behind this is the PVA layer, which is not actually protecting the resist. The PVA layer and its violation of functionality is discussed in Section. 3.4.

SEM images of *AMIL* exposures with thin resist (Shipley S1813 positive photoresist of thickness ~70nm) in the stack are shown in Figs. 3.6 (a) and (b). For both the exposures, λ_1 = 310nm and λ_2 = 633nm and their respective intensities are 25.06μW/cm^2 and 7.04mW/cm^2 are the same. But doses are 21 hours and 7 hours, respectively. Grating seen here is very shallow of only a few nanometres when compared to thick resist samples.

More AFM images of recent *AMIL* exposures are shown in Fig. 3.7. This time along with thicker resist, we tried exposures without ARC in the stack and also did exposures with very thin resist by going all the way down to 30nm by thinning Shipley

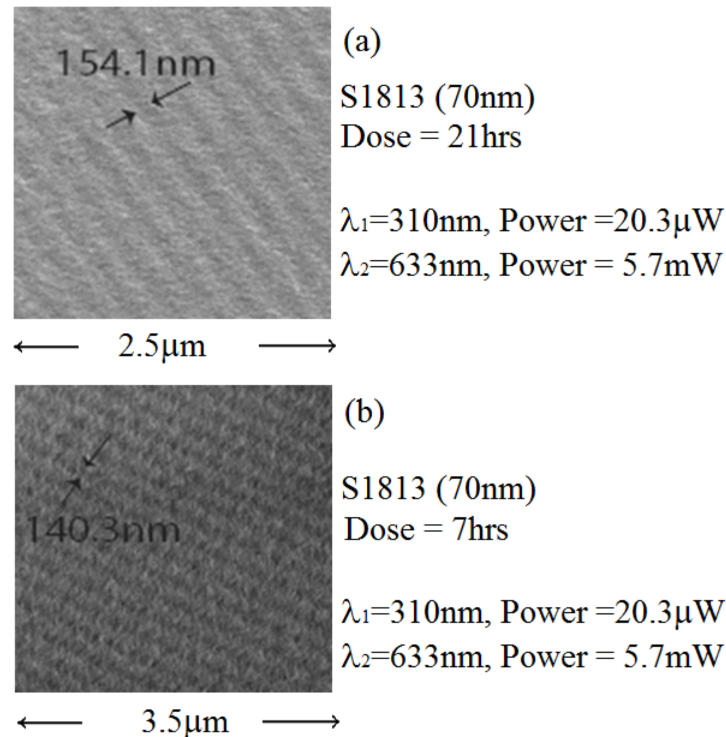

Figure 3.6: SEM images of *AMIL* exposures (thin resist = 70nm) with BTE as AML

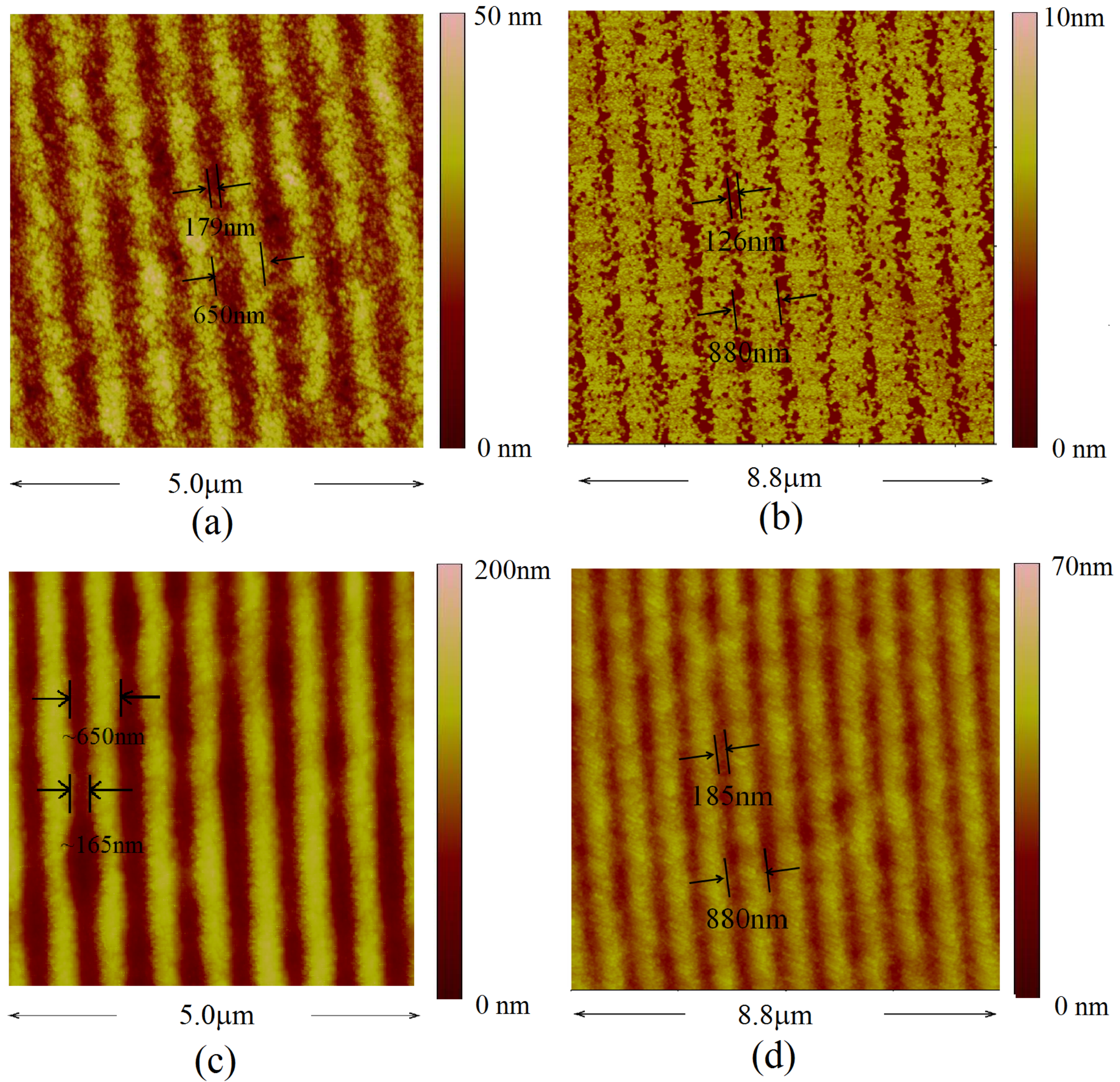

Figure 3.7: More AFM images of *AMIL* exposures with BTE as AML

S1813 in the ratio of 1 : 11 in Thinner P and then spun-coated at very high rpm on a spinner. Even the exposures with thinner resist (30nm), stack does not have ARC, but to improve adhesion, HMDS is spun-coated before putting resist in the stack. Moreover, thermal annealing of BTE is done on all these samples which might be the reason for seeing repetitive reasonably good grating with thick/thinner resist.

In Fig. 3.7, (a) and (c) correspond to *AMIL* exposures of samples with thicker resist (Shipley S1813 of thickness 1.58μm), whereas (b) and (d) correspond to *AMIL* exposures of samples with thinner resist (30nm). Moreover, both PVA and BTE layers

are thermally annealed by heating the sample on a hotplate at 80°C for 90 seconds and then in an oven at 110°C for 1 hour, respectively. Significant betterment in exposure roughness is seen after including this thermal annealing step in the sample preparation procedure. Thus, this could be one of the possible solutions for the comparative roughness seen earlier.

The purpose of preferring thin resist samples is that narrow linewidth is possible and also exposure doses are very much less for the thinner resist samples compared to thicker resist samples, which means lot of time is saved by adopting the thinner resist even though aspect ratio of the grating is good for the thicker resist samples. To even enhance the exposure dose (decrease), chemically amplified resist can be used, but it goes bad very soon when compared to other resist samples.

3.5.2 Diarylethene Polymer as Absorbance Modulation Layer

In this subsection, for all the *AMIL* exposures, samples used had Diarylethene polymer as an absorbance modulation layer(AML) in the stack of layers instead of BTE. More about this polymer including funtionality, absorbance curves through UV-Vis measurements, *etc* are discussed in Chapter 2.

AMIl exposures corresponding to thicker resist(undiluted Shipley S1813 positive photoresist of thickness 1.58μm) samples with Diarylethene polymer as AML in the stack are shown in Fig. 3.8. Among these AFM images, (a) and (b) correspond to the same exposure dose (2 hours 40 minutes), and the same source wavelengths, $\lambda 1$ = 310nm and $\lambda 2$ = 633nm. Intensity of λ_2 is 2.42mW/cm^2 and of λ_1 is 8.27μW/cm^2. The only difference is they are developed in diluted TMAH (developer solution) for 5 and 10 seconds, respectively. Fig. 3.8 (c) and (d) also correspond to similar exposures explained earlier with wavelength sources λ_1 = 310nm and λ_2 = 633nm of same intensity 2.90mW/cm^2. But intensity of $\lambda 1$ are 4.815μW/cm^2 and 0.3086μW/cm^2, respectively. Since ratios are way different, correspondingly doses of these two exposures are 290 and 2390 minutes, respectively.

From Fig. 3.8, it is evident that with a small change in developer time we saw change in linewidth, which means that a lot of calibration is needed for the precise development time, exposure dose visible in (a) and (b). The same concept without

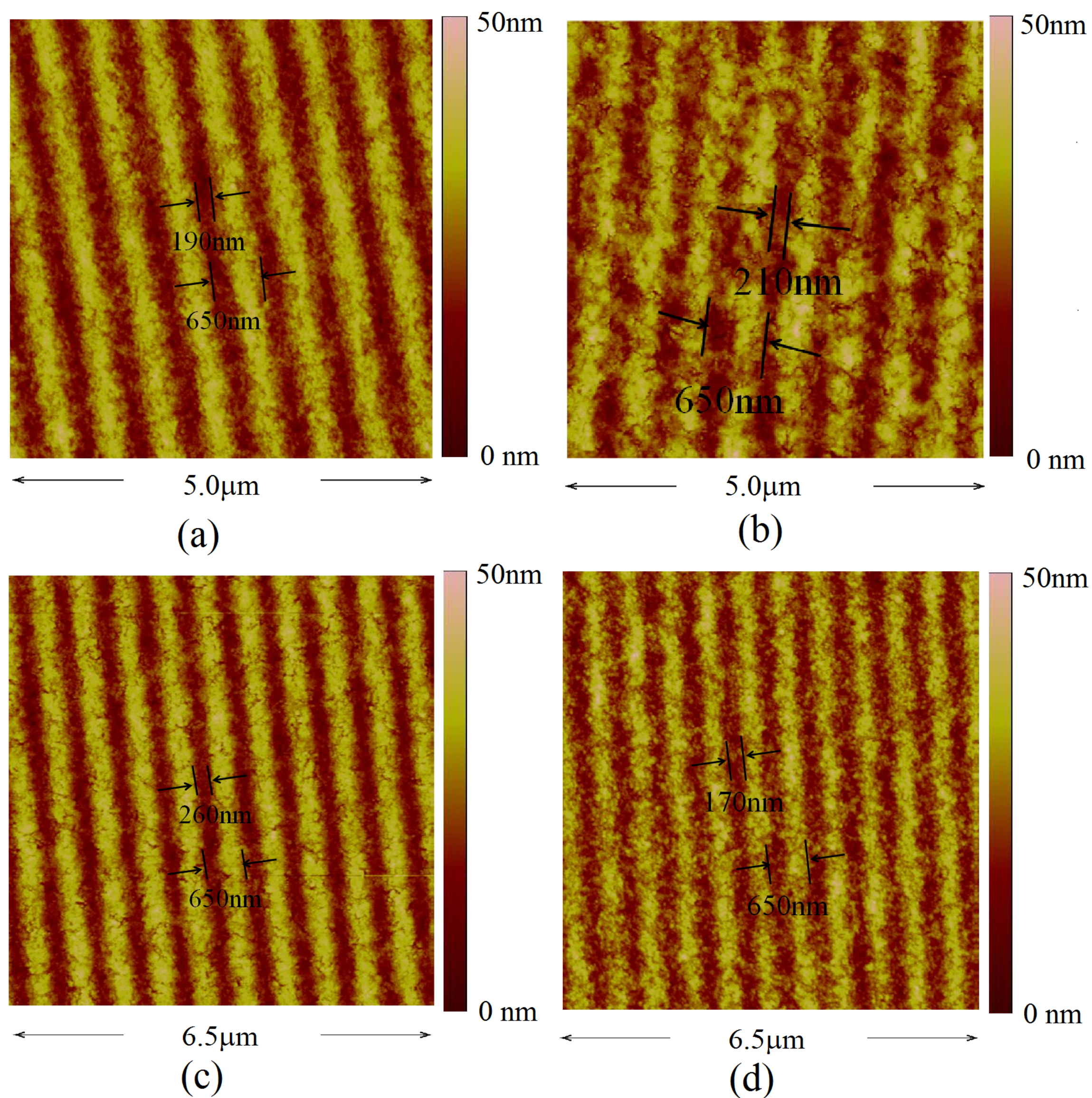

Figure 3.8: AFM images of *AMIL* exposures with Diarylethene polymer as AML

changing setup, development time, change in linewidth *w.r.t* change in exposure dose can be observed in subsection. 3.5.3. From (c) and (d) it is evident that linewidth is primarily based on **source wavelengths intensity ratio** and exposure dose **but not on the wavelengths of the source**.

Moreover, with these photochromic molecules we were also able to see grating under certain exposure doses and source intensity ratios. By the time we attempted

to try it on thinner resist(30nm) samples, we were short of this polymer, so exposures on thinner resist are only with BTE.

3.5.3 Linewidth *vs.* Dose

One of the *AMIL* exposures performed on the sample with diarylethene polymer is extended further to see the change in linewidth *w.r.t* exposure dose, provided remaining parameters are constant among these exposures, shown in Fig. 3.9. Layers in the stack of the sample used for this exposure are ARC (1.25μm), Shipley S1813 photoresist (1.58μm), pva (10nm) and Diarylethene polymer (400nm). Intensities of λ_1 and λ_2 are 0.27μW/cm^2 and 2.9mW/cm^2, respectively. Figs.(a)-(f) in 3.10 correspond to AFM images of exposures whose doses are in a descending order and also of the linewidth is observed.

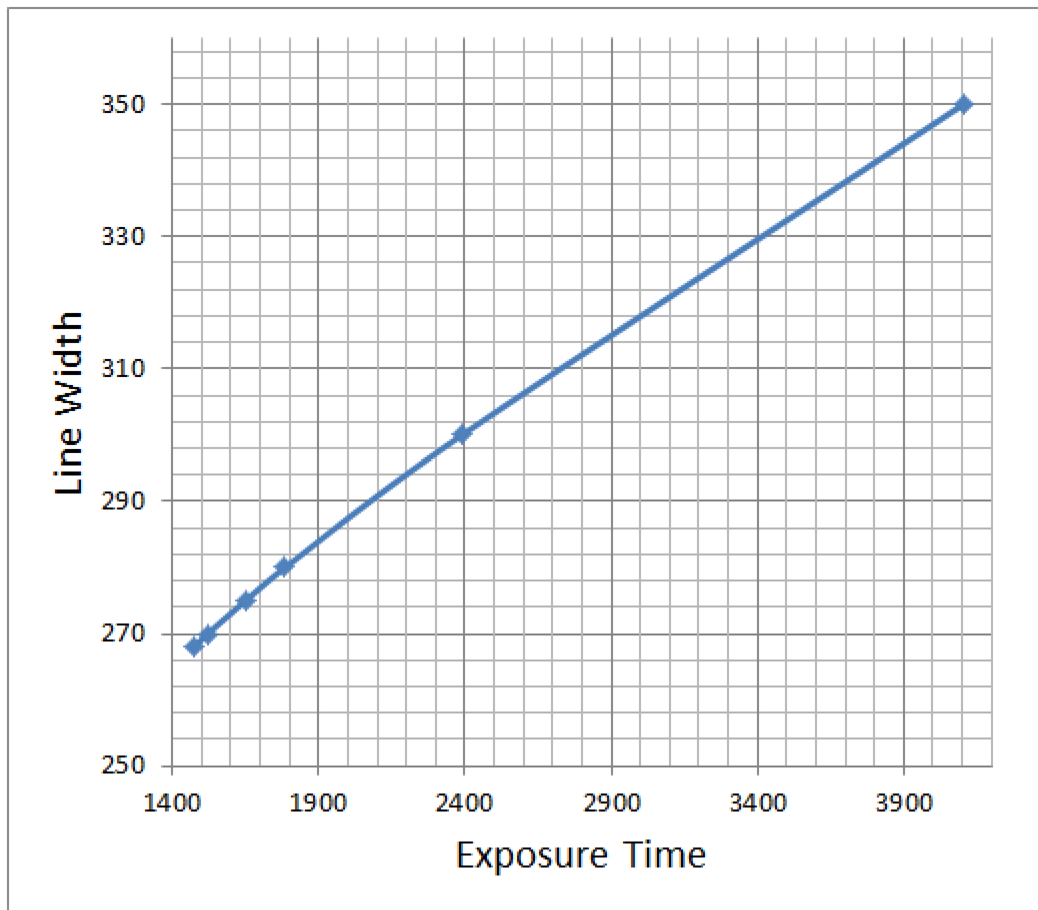

Figure 3.9: Graph corresponds to line width versus single *AMIL* exposure dose

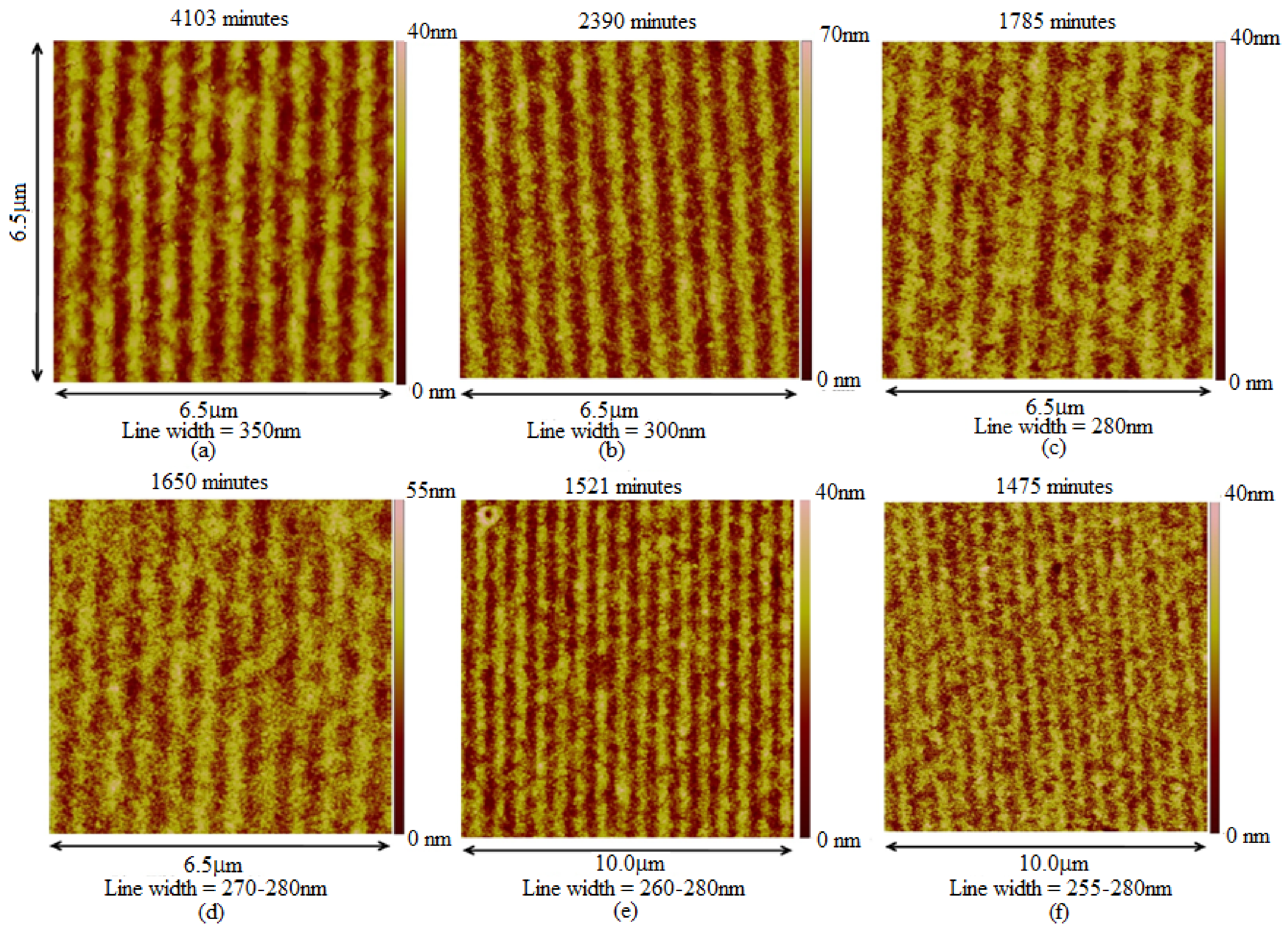

Figure 3.10: AFM images of different *AMIL* exposures with same intensity ratio of λ_1 and λ_2, period of the grating is 650nm

Graphical representation of linewidth of the grating *versus* exposure dose is shown in Fig. 3.9. Exposure time is reported along the x-axis, and linewidth along the y-axis. From the graph, linewidth varies linearly with the exposure dose. Linewidth measurements corresponding to exposure doses are tabulated in Table. 3.1.

Table 3.1: Linewidth *vs.* exposure time of a single AMIL exposure.

Exposure	Exposure time(minutes)	Linewidth(nm)
1	4103	350
2	2390	300
3	1785	280
4	1650	275
5	1521	270
6	1475	267.5

CHAPTER 4

CONCLUSIONS

The complexity of today's VLSI designs demands vast improvements in lithography as well. Significant improvements in lithography are also a major factor in driving Moore's Law so far. Lithography using mask is hindered by many factors in attempting to attain smaller resolutions in nanoscale. In this regard, maskless lithography is gaining a lot of importance especially to meet the industrial demand. Even though huge research is going on, no cost effective maskless lithography replaced Scanning Electron-Beam Lithography(SEBL), Focused Ion Beam (FIB), etc. The proposed research is an attempt to enhance the current ways of patterning that can be used for large scale production especially in terms of cost perspective which is a major concern in the current economy. The proposed research is expected to make significant contributions in the semiconductor industry.

4.1 Summary

This thesis presents a novel optical lithography technique that has the ability to overcome the diffraction limit. From the results, discussed in Chapter 3, it is evident that it can create the pattern exceeding the Abbe's diffraction limit.

This research is a simple technique when compared to conventional Scanning Electron-Beam Lithography(SEBL) or Focused Ion Beam (FIB), which are very complex systems, and also attaining parallelism is extremely challenging. Moreover, this *AMIL* is an easy means to create periodic pattern. With increasing the intensities of both the wavelength sources, exposures are much faster. Hence four major contributions of this study are:

- Effective approach for creating miniature patterns exceeding the diffraction barrier.

- Minimal placement errors when compared to most of the other maskless lithography techniques that are based on charged particles.
- Simple and cost effective system when compared to conventional SEBL or FIB
- A fast way to create miniature pattern over the large area

4.2 Future Work

This research is an alternative to create the miniature periodic pattern over a large area which is almost impossible with many other maskless lithography methods. Problems associated with this technique are discussed in Chapter 3 but still there is a significant scope for research in this area. The major research directions in this area are :

- New setup with high power sources.
- Other photochromic molecules that have even better absorbance contrast.
- Use of chemically amplified resist.
- More multiple exposures.
- AML that does not affect the resist.
- Pattern transfer

4.2.1 New Setup with High Power Sources

Even though this technique is described as a faster way to create miniature pattern, but actually during the research, it takes several hours sometimes days to do just a single exposure due to the fact that we need higher intensity ratio of λ_2 and λ_1 for smaller line widths. Since we are limited by intensity of λ_2, we are forced to reduce the λ_1 intensity such that ratio of intensities is still high. Eventually because of low λ_1, the resist is taking a very long time to expose. To avoid this we have to increase the intensity of λ_2 such that even with increasing intensity of λ_1, we can still achieve a very high ratio, and because the λ_1 intensity is high, resist is exposed much faster and hence at a lesser exposure dose.

4.2.2 Other Photochromic Molecules that Have Even Better Absorbance Contrast

It is unquestionable that BTE or Diarylethene polymer (photochromic molecules) is the primary layer that is responsible for this absorbance modulation. In future, any photochromic molecules that have even better contrast in UV and Red will lead to even better grating, because the higher the absorbance contrast the better the layer acts as an ideal mask in the portions where it is supposed to be. Hence features are infinitely better even on thin resist.

4.2.3 Use of Chemically Amplified Resist

Another alternative to improve the expose dose (minimal) of this *AMIL* technique is to use a chemically amplified resist. A few exposures discussed in Chapter 3 are based on chemically amplified resist (TDUR). These exposures are much faster when compared to ones exposed with ordinary Shipley s1813 resist. The only problem associated with these resists is that they easily go bad or get contaminated upon exposure to air for a long time, thus making them not appropriate to use everywhere.

4.2.4 More Multiple Exposures

Due to limitations caused by the nanopositioning peizo-controlled stage, precise control over the stage movement has been a problem, ending up with a trial and error concept in moving the stage manually and then determining the displacement from the results. Based on the photochromic molecule, for a certain amount of time the sample is exposed to only λ_2 until molecules are converted back to original form. More than two exposures can be demonstrated.

4.2.5 AML that Does Not Affect the Resist

The purpose of the PVA layer to is to block or protect the resist layer from the top which is photochromic molecules in our case. If the AML is not attacking the resist, then the PVA layer can be excluded in the stack. This can be done by choosing a solvent to mix the photochromic molecules. For instance, Diarylethene polymer mixed in chloroform will attack the resist if it is spun coated on top of the resist. If

Diarylethene polymer is mixed in toluene and then spun coated, it will not attack the resist because toluene does not affect the resist.

4.2.6 Pattern Transfer

The ultimate goal behind patterning the resist is to transfer the pattern onto the underlying layer of photoresist, which in this research would be Silicon. Once pattern is created using AMIL, it can be easily transferred to the underlying layer (Silicon) using conventional etching techniques which are not yet limited by the current nanoscale requirements. Outline of the pattern transfer onto Silicon substrate is shown in Fig. 4.1

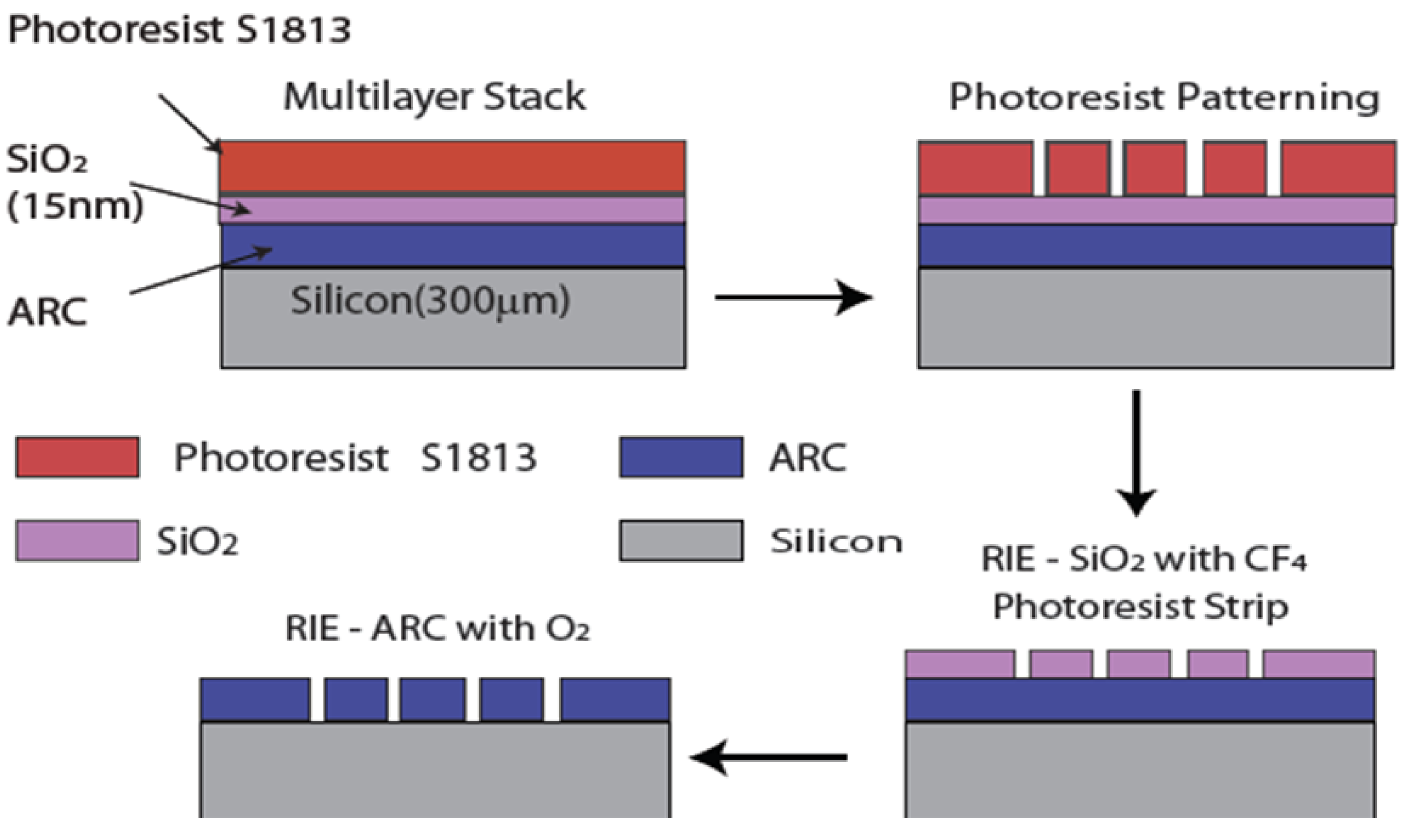

Figure 4.1: Pattern transfer outline. The purpose of the Silicon-dioxide layer is to transfer the pattern onto ARC.

REFERENCES

[1] R. F. Pease and S. Y. Chou, “Lithography and other patterning techniques for future electronics,” in *Proceedings of the IEEE*, vol. 96, Feb. 2008, pp. 248-270.

[2] B. La Fontaine, “Lasers and Moores Law,” in *SPIE Professional*, Oct. 2010, pp. 20-28.

[3] G. E. Moore, “Lithography and the future of Moore’s law,” in *Proceedings of the SPIE*, vol. 2438, Feb. 1995, pp. 2-14 [DOI:10.1117/12.210341].

[4] S. Okazaki, “Resolution limits of optical lithography,” in *IEEE: Journal of Vacuum Science & Technology B: Microelectronics and Nanometer Structures*, vol. 9, Nov. 1991, pp. 2829-2833.

[5] L.R. Harriott, “Limits of lithography,” in *IEEE: Proceedings of the IEEE*, vol. 89, March 2001, pp. 366-374.

[6] [Online] Micron Technology Company website http://www.micron.com/products/solid_state_storage/client_ssd.html

[7] R. Menon, A. Patel, D. Gil, and H. I. Smith, “Maskless lithography,” in *Materials Today*, Feb. 2005, pp. 26-33.

[8] J. T. Hastings, F. Zhang, and H. I. Smith, “Nanometer-level stitching in raster-scanning electron-beam lithography using spatial-phase locking,” in *American Vacuum Society: Journal of Vacuum Science & Technology B: Microelectronics and Nanometer Structures*, vol. 21, Dec. 2003, pp. 2650-2656.

[9] J. A. Liddle, G. M. Gallatin and L. E. Ocola, “Resist requirements and limitations for nanoscale electron-beam patterning,” in *Material Research Society: Symposium Proceedings*, vol. 739, Jan. 2003, pp. 19-30.

[10] M. E. Walsh and H. I. Smith, “Method for reducing hyperbolic phase in interference lithography, in *Journal of Vacuum Science & Technology B: Microelectronics and Nanometer Structures*, vol. 19, Nov. 2001, pp. 2347-2352.

[11] T. A. Savas, M. L. Schattenburg, J. M. Carter and H. I. Smith, “Large-area achromatic interferometric lithography for 100 nm period gratings and grids,” in *American Vacuum Society: Journal of Vacuum Science & Technology B: Microelectronics and Nanometer Structures*, vol. 14, Nov. 1996, pp. 4167-4170.

[12] M. E. Walsh, Y. Hao, C. A. Ross and H. I. Smith, “Optimization of a lithographic and ion beam etching process for nanostructuring magnetoresistive thin film stacks,” in *American Vacuum Society: Journal of Vacuum Science & Technology B: Microelectronics and Nanometer Structures*, vol. 18, no. 6, Nov. 2000, pp. 3539-3543.

[13] P. T. Konkola, C. G. Chen, R. K. Heilmann, C. Joo, J. C. Montoya, C. Chang and M. L. Schattenburg, "Nanometer-level repeatable metrology using the nanoruler, in *American Vacuum Society: Journal of Vacuum Science & Technology B: Microelectronics and Nanometer Structures*, vol. 21, no. 6, Nov. 2003, pp. 3097-3101.

[14] S. Kramer, R. R. Fuierer and C. B. Gorman, "Scanning probe lithography using self-assembled monolayers," in *American Chemical Society: Chemical Reviews*, vol. 103, no. 11, June 2003, pp. 4367-4418.

[15] D. S. Ginger, H. Zhang and C. A. Mirkin, "The evolution of dip-pen nanolithography," in *Angewandte Chemie International Edition*, vol. 43, no. 30, Nov. 2003, pp. 2683-2688.

[16] T. Sandstrom, A. Bleeker, J. Hintersteiner, K. Troost, J. Freyer and K. V. Mast, "OML: Optical maskless lithography for economic design prototyping and small-volume production," in *Proceedings of the SPIE*, vol. 5377, May 2004, pp. 777-787.

[17] N. Choksi, D. S. Pickard, M. McCord, R. F. W. Pease, Y. Shroff, Y. Chen, W. Oldham and D. Markle, "Maskless extreme ultraviolet lithography," in *American Vacuum Society: Journal of Vacuum Science & Technology B: Microelectronics and Nanometer Structures*, vol. 17, no. 6, Sep. 1999, pp. 3047-3051.

[18] T. H. P. Chang, M. Mankos, K. Y. Lee and L. P. Muray, "Multiple electron-beam lithography," in *Micro- and Nano-Engineering 2000: Microelectronic Engineering*, vol. 57, Sep. 2001, pp. 117-135.

[19] R. F. Pease, L. Han, G. I. Winograd, W.D. Meisburger, D. Pickard and M. A. McCord, "Prospects for charged particle lithography as a manufacturing technology," *Microelectronic Engineering*, vol. 53, no. 4, June 2000, pp. 55-60.

[20] C.N. Berglund, "Electron-beam direct-write for IC fabrication," *Microelectronic Manufacturing and Testing*, vol. 23, May 1989, pp. 39-52.

[21] M.A. McCord,"Electron beam lithography for 0.13 μm manufacturing," in *Journal of Vacuum Science and Technology B: Microelectronics and Nanometer Structures*, vol. 15, no. 6, April 1997, pp. 2125-2129.

[22] M. E. Walsh, "On the design of lithographic interferometers and their application," *PhD Thesis*, MIT, Sep. 2004.

[23] R. Menon and H. I. Smith, "Absorbance-modulation optical lithography," in *American Vacuum Society: Journal of Vacuum Science & Technology A*, vol. 23, no. 9, Mar. 2006, pp. 2290-2297.

[24] M. Irie, *American Chemical Society: Chemical Reviews*, vol. 100, June 2000, pp. 1685-1690.

[25] N. Katsonis, T. Kudernac, M. Walko, S. J. V. Molen, B. J. VanWees and B. L. Feringa, "Reversible conductance switching of single diarylethenes on a gold surface," in *Advanced Materials*, vol. 18, no. 11, May 2006, pp. 1397-1400.

[26] R. Menon, H.-Y. Tsai, and S.W. Thomas III, "Far-field generation of localized light fields using absorbance modulation," in *Physical Review Letters*, vol. 98, Jan. 2007, pp. 1-4.

[27] H. Ishii, S. Usui, K. Douki, T. Kajita, H. Chawanya and T. Shimokawa, "Design and lithographic performances of 193-specific photoacid generators," in *Proceedings of the SPIE*, vol. 3999, Sep. 2000, pp. 1120-1132.

[28] "UV-Visible Spectroscopy," *Cem.msu.edu*, Retrieved 2010-02-26.

[29] M. Braun, F. Gruber, M. Ruf, S. Kumar, E. Illenberger and H. Hotop, "IR photon enhanced dissociative electron attachment to SF6: Dependence on photon, vibrational, and electron energy," in *Chemical Physics*, vol. 329, Nov. 2006, pp. 148-156.

[30] C. A. Mack, *Fundamental Principles of Optical Lithography the Science of Microfabrication*, Chichester, West Sussex, England: *Wiley*, 2007.